

10504 5914 NT ACVN
NACA TN 4165

0067024



TECH LIBRARY KAFB, NM

NATIONAL ADVISORY COMMITTEE FOR AERONAUTICS

TECHNICAL NOTE 4165

THERMAL FATIGUE OF DUCTILE MATERIALS

II - EFFECT OF CYCLIC THERMAL STRESSING ON THE
STRESS-RUPTURE LIFE AND DUCTILITY

OF S-816 AND INCONEL 550

By Francis J. Clauss and James W. Freeman

Lewis Flight Propulsion Laboratory
Cleveland, Ohio



Washington

September 1958

AFM C
TECHNICAL
AFL 2011

NATIONAL ADVISORY COMMITTEE FOR AERONAUTICS



0067024

TECHNICAL NOTE 4165

THERMAL FATIGUE OF DUCTILE MATERIALS

II - EFFECT OF CYCLIC THERMAL STRESSING ON THE STRESS-RUPTURE

LIFE AND DUCTILITY OF S-816 AND INCONEL 550*

By Francis J. Clauss and James W. Freeman

SUMMARY

An experimental study was made of the changes in the stress-rupture life, ductility, hardness, and microstructure of S-816 and Inconel 550 specimens that had been exposed to varying amounts and conditions of thermal fatigue.

Tensile specimens of S-816 and Inconel 550 were alternately heated and cooled while constrained in a manner that prevented their free axial expansion and contraction. Before failure by thermal fatigue occurred, the thermal cycling was discontinued so that the effect of the number of cycles on the properties of the material could be measured. The thermal cycling covered a range of maximum cycle temperature, temperature difference in cycling, and cyclic exposure time at the maximum cycle temperature. A few specimens were first run for short periods of time in stress-rupture and were then failed by thermal fatigue.

Exposure to thermal-fatigue conditions strengthened S-816 in stress rupture and weakened Inconel 550. Under the most damaging conditions studied, Inconel 550 lost 98 percent of its original stress-rupture life as a result of prior thermal fatigue, even though the number of cycles was only one-half of that required for failure by thermal fatigue alone. The stress-rupture life of S-816 was increased by about 50 percent. When specimens were first exposed to stress-rupture conditions and then run to failure in thermal fatigue, the thermal-fatigue life of S-816 was sharply reduced, whereas that of Inconel 550 showed a slight increase. The results can be interpreted by extending existing theories of mechanical fatigue and creep-rupture to thermal fatigue.

*The information presented in this report was offered by Dr. F. J. Clauss as a thesis in partial fulfillment of the requirements for the degree of Doctor of Philosophy in Metallurgical Engineering, University of Michigan, Ann Arbor, Michigan, June 1957. Professor James W. Freeman was chairman of Dr. Clauss' doctoral committee and is also a consultant to the Lewis Flight Propulsion Laboratory.

INTRODUCTION

In the first part of the study of the thermal-fatigue process in ductile materials, a study was made of the effect of the maximum cycle temperature, the temperature difference of cycling, the cyclic time of exposure at the maximum cycle temperature, and the cyclic plastic strain on the number of cycles to fracture (ref. 1). Presumably exposure to thermal-fatigue conditions might weaken a material so that it would fail in service from other loading stresses long before it would fail as a result of thermal fatigue alone. On the other hand, the strain- and/or precipitation-hardening that occurred during constrained thermal cycling might strengthen a material. The purpose of this investigation was, therefore, to study the changes in the stress-rupture life and ductility of materials that had been exposed to varying amounts and conditions of thermal fatigue, where the number of cycles was insufficient to cause fracture by thermal fatigue alone. Besides providing useful engineering data, such information can also be helpful in understanding and developing a theory for the mechanism of thermal fatigue.

EQUIPMENT AND PROCEDURE

The equipment and procedure were essentially the same as in reference 1; that is, tensile specimens of S-816 and Inconel 550 were alternately heated and cooled while constrained in a manner that prevented their free axial expansion and contraction. However, instead of continuing the heating and cooling until the specimens fractured, the thermal cycling was interrupted at an earlier time and the specimens were then removed from the gripping block and examined metallographically or tested in stress-rupture. In these cases, the bolts constraining the specimens were loosened after the desired number of cycles while the temperature was at a minimum of 200° F. Thus, all of these specimens were removed just after having been subjected to a tensile stress at the same temperature. Most of the thermal cycling was done with a maximum temperature T_{max} of 1350° F and a minimum temperature T_{min} of 200° F, using a cycle of 30 seconds of heating to T_{max} , 15 seconds at T_{max} , 30 seconds of cooling to T_{min} , and 15 seconds at T_{min} . In some tests the holding time at T_{max} was increased to 60 seconds. In other tests, a range of T_{max} from 1250° to 1550° F was studied.

4671

In specimens removed for stress-rupture testing, the test sections were ground to a depth of about 0.002 to 0.004 inch below the original specimen diameter to remove any bulges and any surface defects that might influence the stress-rupture strength. All of these specimens were examined by zygo after being ground, and in no cases were any surface cracks detected. Threads were also ground on the end shoulders for holding the specimens in the stress-rupture machines. Stress-rupture tests were conducted principally at 1350° F, although one series of S-816 specimens was tested at 1500° F. The stresses were selected to cause failure in roughly 100 hours on virgin material. Both time to rupture and reduction in area at the fracture were determined. Figure 1 shows stress-rupture failures of virgin material.

Some specimens were thermally cycled without constraint in order to observe any changes in properties that might be due to temperature conditions alone.

CA-1 back

Specimens for metallographic study were prepared by carefully machining flat surfaces through a central plane along the tensile axes. Hardness was measured with a microhardness tester, using a Vickers diamond penetrator and a 1-kilogram load.

A few specimens were first run for short periods of time in stress-rupture and were then failed by thermal fatigue. The surfaces of the test sections of these specimens were lightly polished before being run in thermal fatigue in order to remove any surface defects produced during exposure to stress-rupture conditions.

An attempt was made to eliminate the effects of bar-to-bar variations in properties by running all tests in a single series from the same bar of material. All data plotted in a single graph in this report refer to results from the same bar of material, or from bars that were shown to have equivalent properties.

RESULTS

Effect of Number of Cycles of Thermal Fatigue

The effect of the number of cycles of thermal fatigue N on the subsequent stress-rupture life and ductility varied markedly with the alloy. For S-816 there was an initial increase in the rupture life at 1350° F (fig. 2(a)). This is shown by the lives of the three specimens cycled 500, 1000, and 1250 times (approx. 21, 42, and 53 percent of the number of cycles that would cause failure by thermal fatigue alone N_f). Beyond 1250 cycles, the data scattered widely. Three specimens had lives greater than the average life of the virgin material (1750, 2200, and 2300 cycles), and the other two specimens had lives slightly less

than the average life of the virgin material (1500 and 2000 cycles). Even the specimen of lowest life (2000 cycles), however, did not have a life significantly below that of the virgin material. From this, one can conclude that there was no significant loss in the rupture life of S-816 at 1350° F due to prior thermal fatigue for the conditions shown, even though cycling was continued to approximately 98 percent of N_f . Figure 2(b) shows the same behavior in the rupture life at 1500° F as a function of the number of prior cycles of thermal fatigue.

For Inconel 550, the rupture life dropped as N was increased (fig. 2(c)). The drop was most rapid at first, then slowed down so that the relation between the stress-rupture life and N was approximately linear. The specimen with the greatest number of cycles prior to a stress-rupture testing ($N = 9000$ cycles = 86.5 percent of N_f) suffered a loss of about one-third of the life of virgin Inconel 550. With the exception of the specimen that had been run 5000 cycles, the data showed little scatter from the curve.

The ductility of S-816 decreased linearly with N (figs. 3(a) and (b)). After about 98 percent of the number of cycles required to fracture S-816 by thermal cycling alone, the reduction in area of specimens fractured in stress-rupture at 1350° F had dropped to about one-half or two-thirds of that for virgin material. There appeared to be no change in the ductility of Inconel 550 during thermal cycling (fig. 3(c)). The decrease in the ductility of S-816 was accompanied by an increase in hardness, as shown in figure 4(a), whereas there was no change in the hardness of Inconel 550 with the number of cycles (fig. 4(b)).

For both S-816 and Inconel 550, no changes due to temperature cycling in the absence of constraints were observed in the stress-rupture life of ductility at 1350° F (figs. 5 and 6).

The microstructure of an S-816 specimen that had been cycled in thermal fatigue and then fractured in stress-rupture at 1350° F is shown in figure 7. This specimen had been cycled 1175 times between 1350° and 200° F, which is one-half of the number of cycles for failure by thermal fatigue alone under these conditions. Comparison of this structure with that of the specimen of virgin material fractured in stress-rupture at the same stress and temperature (fig. 1(a)) shows that there was considerable additional precipitation during thermal fatigue and that the grains were less elongated in the thermally cycled specimen than in the virgin material.

The loss in strength of Inconel 550 during cycling appears to correlate with its microstructural behavior. Thus, thermal cycling the Inconel specimens between 1350° and 200° F caused the grain boundaries to fragment, as shown in figures 8(a) to (c). Figure 8(a) shows a grain boundary running from the junction of three grains. The original boundary

appears to be broken into smaller segments that are offset from one another. The axis of the specimen was approximately as indicated, and this specimen was removed after only 1000 cycles, or about one-tenth of its expected life. Figure 8(b) shows the same area as figure 8(a), but at a lower magnification. Figure 8(c) is another example of grain-boundary fragmentation. This specimen was removed after 7000 cycles, or seven-tenths of its expected life. Note the extreme amount by which the grain boundary was displaced near the bottom of the photomicrograph.

An example of deformation by twinning is shown in figure 8(d). The twin lines run at a slight angle to the axis of the specimen, and what appear to be small cracks are seen at the ends of those twin lines that are more nearly perpendicular to the axis. This specimen was removed after 2000 cycles (approx. two-tenths of N_f). Several other examples of deformation within the grains are shown in figures 8(e) and (f). The specimen is the same for these last two figures and was removed after 7000 cycles (seven-tenths of N_f).

Microstructural damage (e.g., a crack) starts in Inconel 550 after fewer cycles than in S-816, but it apparently propagates more slowly in Inconel 550. As a result, Inconel 550 endures more cycles of thermal fatigue under these conditions than does S-816.

Effect of Time at Maximum Cycle Temperature

The effect of time at a T_{max} of 1350° F was studied by increasing the time at T_{max} from 15 to 60 seconds. From the results described in reference 1, this increase at a T_{max} of 1350° F had little effect on N_f for S-816 (fig. 17(b), ref. 1), but caused N_f for Inconel 550 to decrease from 10,500 to 7,400 cycles (fig. 17(a), ref. 1).

As with the shorter cycle, the rupture life of S-816 increased with the number of cycles (at least up to $N = 1/2 N_f$), and that of Inconel 550 decreased (fig. 9). Although the curve is not well defined because of scatter, the drop in the life of Inconel 550 appears to be more rapid than on the shorter cycle, and failure was reached in fewer cycles. The ductility of Inconel 550 remained constant as N increased; S-816 also retained the same ductility up to 1000 cycles (fig. 10), whereas there was a loss in ductility with N on the shorter cycle (fig. 3(a)).

Effect of Maximum Cycle Temperature

The effect of T_{\max} was studied by removing specimens for rupture testing after one-half of the number of cycles that would cause failure by thermal fatigue alone. The effect of T_{\max} on the subsequent properties differed considerably between the two alloys.

The stress-rupture life of S-816 after thermal fatigue was about 50 percent greater than that of the virgin material regardless of T_{\max} (for the range of T_{\max} from 1250° to 1550° F), provided that cycling was stopped at $1/2 N_f$ (fig. 11(a)). The stress-rupture life of a single specimen of S-816 cycled without constraint between the highest T_{\max} (1550° F) and a T_{\min} of 200° F (solid triangle, fig. 11(a)) was also slightly greater than that of virgin material, although the increase here was less than that for constrained cycling and could be due to scatter. Inconel 550, on the other hand, suffered a drastic loss in strength as T_{\max} was increased (fig. 11(b)); at a T_{\max} of 1550° F about 98 percent of its original stress-rupture life was lost. This loss was not due to temperature alone, as shown by the single specimen cycled without constraint between a T_{\max} of 1550° F and a T_{\min} of 200° F (solid triangle, fig. 11(b)), and the loss of strength must, therefore, have been due to the combined effects of the cyclic stresses (or strains) and temperatures. As shown in figure 12, the ductility of S-816 cycled under constraint did not vary consistently with T_{\max} , but the individual values scattered about the ductility of the virgin material. The ductility of Inconel 550 cycled under constraint remained constant, regardless of cycling over the range of T_{\max} studied. However, without constraint, temperature cycling at the high T_{\max} of 1550° F resulted in a slight increase in the ductility of both materials.

Specimens of the two alloys that had been cycled both with and without constraint between 1550° and 200° F for one-half the number of cycles for failure by thermal fatigue alone and then fractured in stress-rupture are shown in figures 13 and 14. For S-816, cycling under constraint caused a marked increase in fine precipitation along slip planes and an increase in the stress-rupture life; there was also less grain elongation than in the virgin material (fig. 13(a)). When the constraint was absent, however, thermal cycling caused little change in the subsequent microstructural behavior (compare figs. 13(b) and 1(a)).

For Inconel 550, cycling under constraint between the same temperature limits introduced considerable void formation, both within the grains and along the grain boundaries, as is shown in figure 14(a). Again, failure was predominantly through the grain boundaries, as in the virgin

material (fig. 1(b)), but the stress-rupture life was markedly reduced. On the other hand, thermal cycling without constraint produced little or no change in the structure and life (compare figs. 14(b) and 1(b)).

Specimens Run in Stress-Rupture, Then Failed by Thermal Fatigue

Only a single group of specimens was first run in stress-rupture and then failed by thermal fatigue. The stress-rupture conditions were a temperature of 1350° F and a stress that would cause the virgin material to fail in roughly 100 hours. Specimens were removed from the stress-rupture test after various periods of time less than that for failure, and they were then cycled to failure in thermal fatigue at 1350° and 200° F. The results for these conditions are plotted in figure 15. For S-816, N_f decreased as the prior time in stress-rupture increased (fig. 15(a)), and for Inconel 550, N_f appeared to increase slightly with the prior time in stress-rupture (fig. 15(b)).

DISCUSSION

The study of the effect of variations in the temperature cycle on the thermal-fatigue life of S-816 and Inconel 550 demonstrated that the temperature level of thermal cycling exerts an important influence on the thermal-fatigue life of ductile alloys (ref. 1). For the materials and test conditions covered, the maximum cycle temperature had more effect than the temperature difference on the number of cycles to failure. Increasing the time of exposure at T_{max} during cycling either increased or decreased the number of cycles to failure, depending upon T_{max} . Thus an increase in time at low T_{max} reduced the thermal-fatigue life, whereas the same increase in time at high T_{max} increased the thermal-fatigue life. No direct correlation existed between the number of cycles to failure and the amount of plastic strain per half cycle.

Long before a specimen fails in thermal fatigue alone, its mechanical properties can be significantly altered. In the present study the stress-rupture strength of S-816 was increased by prior thermal fatigue, whereas that of Inconel 550 was reduced. The increase in the stress-rupture life of S-816 was usually accompanied by a loss of ductility. Exposure to stress-rupture conditions decreased the subsequent thermal-fatigue life of S-816 and appeared to increase that of Inconel 550 slightly.

The appendix summarizes pertinent points of existing theories of mechanical fatigue and creep-rupture for the thermal-fatigue process. In applying these theories to thermal fatigue, the fatigue process is assumed to be divided into two stages. The two stages are (1) a stage of strain- and/or precipitation-hardening and (2) a stage of destruction of cohesive

bonds and development and propagation of cracks. Each of these stages can proceed at varying rates, depending upon the material and the test conditions. The theory is discussed first for fixed test conditions; in the present work, the conditions of cycling studied most thoroughly were a T_{\max} and T_{\min} of 1350° and 200° F, respectively, in a 30-15-30-15-second cycle.

During the first stage, the strains are absorbed by the material without cracking, and the strength and hardness increase while the ductility decreases. This was true for S-816 under the conditions stated. Thus, for a large number of cycles, S-816 became harder, stronger in stress-rupture, and lower in ductility.

The second stage of fatigue is apparently reached in S-816 only when the number of cycles is near that required for failure by thermal fatigue alone, and then is passed through relatively quickly, as evidenced by the sharp drop in the stress-rupture life when the number of cycles is near that for failure by thermal fatigue alone. On the other hand, the second stage can be reached very early in the fatigue process, as is apparently the case for Inconel 550. Thus, Inconel 550, which is initially harder and less ductile than S-816, does not harden further during cycling; its stress-rupture life drops continually during cycling (abruptly at first, then more gradually, and then abruptly again at the end), and its ductility remains the same.

Several factors might be important in considering the onset of the second stage of fatigue and in accounting for the differences in the behavior of S-816 and Inconel 550. One is that the second stage begins when the ductility of the material is too low to absorb the cyclic strains without cracking. S-816 reaches this stage only after extensive strain-and/or precipitation-hardening in the first stage, while Inconel 550, which is fully hardened by the prior heat treatment and is much less ductile than S-816, seems to be in the second stage of fatigue from the start. This reasoning is in agreement with the hardness behavior during cycling and with the variation in the subsequent stress-rupture behavior of the two alloys. On the other hand, Inconel 550 is a ductile alloy, undergoing a reduction of area of about $7\frac{1}{2}$ percent in the stress-rupture test, and S-816 still has considerable ductility (reduction in area of more than 30 percent) even when the number of cycles is close to that required for failure by thermal fatigue alone. These values would seem to ensure sufficient ductility for the alloys to absorb the cyclic strains without cracking. However, the reduction in area is a gross measurement that does not indicate the actual ductility in those localized regions where plastic deformation during reversed stressing is concentrated. Experimental evidence of the concentration of plastic deformation during thermal cycling of S-816 and Inconel 550 is discussed in reference 1. It appears very likely that, because of this nonuniformity in straining, certain areas

become embrittled and are unable to absorb further cyclic straining without cracking; hence cracks can form during thermal cycling even though the major portion of the material is still quite ductile.

Another factor that might influence the onset of the second stage is the mode of deformation of the material. Inconel 550 shows a tendency to deform in thermal fatigue by twinning, in contrast to simple slip in S-816. Twinning is considered by some to be related to cleavage and brittle fracture (see appendix). Thus the early incidence of micro-cracking in Inconel 550, as evidenced by the microstructural behavior and reflected in the drop in stress-rupture life, might be due to its particular mode of deformation under cyclic strains.

A third factor to be considered is the effect of the particles of precipitate in the alloys (or, more exactly, the effect of the coherency stresses surrounding the particles). The significant points here are that the precipitates can act as barriers to the movement of dislocations and can serve as the sites at which vacancies cluster together to form voids. In this action, the precipitates would promote cracking. However, if the precipitates overage and soften, cracking might be alleviated. The tendencies of different materials to overage depends upon the stability of the precipitates; however, as figure 4 indicates, neither S-816 nor Inconel 550 overages or anneals during cycling to a maximum temperature of 1350° F.

If the separation of the fatigue process into the two stages described is accepted, the behavior of specimens that were first run in stress-rupture at 1350° F for varying times short of fracture and then failed in thermal fatigue between 1350° and 200° F can be interpreted as follows. A specimen of S-816 removed from stress-rupture conditions at 1350° F has used up an appreciable amount of its ductility in creep, and the remaining ductility is less as the time in stress increases. When the specimen is then cycled in thermal fatigue, the first stage is shorted, and the second stage begins in fewer cycles as the prior time in stress increases, that is, as the remaining ductility for absorbing the cyclic strains is decreased. In addition, the specimen can be structurally damaged if the time in stress is sufficiently long for it to begin third-stage creep. As a result, the number of cycles to failure in thermal fatigue should fall off as the prior time in stress is made longer, and this is the effect that was found. Note that this effect for S-816 is exactly opposite to that for the reverse order of testing, where prior thermal fatigue increased the subsequent stress-rupture life.

In contrast to S-816, Inconel 550 creeps very little in a 100-hour stress-rupture test at 1350° F; hence, its available ductility for subsequent thermal fatigue is not markedly diminished. Moreover, the behavior of Inconel 550 has been interpreted to show the absence of a significant first stage of thermal fatigue. Therefore, the number of

cycles to failure in thermal fatigue should not fall off markedly as the prior time in stress-rupture increases, so long as structural damage during third-stage creep is absent. In accordance with this interpretation, the thermal-fatigue life of Inconel 550 does not decrease; in fact, there appears to be a slight increase, perhaps due to secondary effects. Again, the effect is opposite to that for the reverse order of testing.

The next step in understanding thermal fatigue is to consider how the behavior under fixed conditions is modified by changing the test conditions. The two test variables that were studied in this investigation were maximum cycle temperature T_{\max} (1250° to 1550° F) and time at T_{\max} (15 and 60 sec).

The effect of raising T_{\max} on the subsequent stress-rupture life after about one-half of the number of cycles that would cause failure by thermal fatigue alone (fig. 11) is interpreted as follows. S-816 being cycled between 1350° and 200° F apparently does not enter the second stage of fatigue until very near the end of the thermal-fatigue process. Since subsequent loss of stress-rupture life depends upon entering the second stage of fatigue, there should be no direct loss if the cycling is stopped during the first stage. Thus, if cycling between 1350° and 200° F is stopped when $N = 1/2 N_F$, fatigue of S-816 is still far from the second stage. Using this conservative fraction of N_F , one might expect that if a number of specimens of S-816 are cycled between maximum temperatures that are not excessively high and 200° F and if cycling is stopped when $N = 1/2 N_F$, fatigue will not have reached the second stage. As shown in figure 11(a), the strengthening action of strain- and/or precipitation-hardening was preserved up to a T_{\max} of 1550° F, which was the highest T_{\max} studied.

Inconel 550, in contrast to S-816, enters the second stage of fatigue very early in the process. The higher strains, as well as the increased rate of vacancy diffusion and the occurrence of recrystallization which accompany an increase in T_{\max} , should aggravate the cracking. As a result, the stress-rupture life after one-half the number of cycles to failure should fall off with T_{\max} , and this behavior is shown in figure 11(b). Note that this effect of T_{\max} was very pronounced; when T_{\max} equaled 1550° F, the stress-rupture life was only about 2 percent of that of the virgin material.

Further information on the effect of T_{\max} is gained from considering the effect of time at T_{\max} on the subsequent stress-rupture life. This effect can vary with temperature; it was studied here only for a T_{\max} of 1350° F and a T_{\min} of 200° F. For S-816, increasing the time of exposure at this value of T_{\max} from 15 to 60 seconds had little

effect on N_f (fig. 17(b), ref. 1). Comparison of figures 2(a) and 9(a) shows that this increase in time at T_{max} did not affect the general trend in the variation of the stress-rupture life with the number of cycles. For both times of exposure, there was an initial increase, and the increase appeared greater for the longer cycle. This last observation might indicate that an appreciable part of the strengthening was due to precipitation-hardening as well as strain-hardening, with the amount of precipitation-hardening increasing with the time of exposure, as was actually observed in the microstructures of S-816.

For Inconel 550, the increase in the time of exposure at a T_{max} of 1350° F reduced N_f from 10,500 to 7,400 cycles (fig. 17(a), ref. 1). Apparently, the damaging effects depend on time and have more time to operate and decrease N_f on the longer cycle. The time dependency of this damaging effect is also clearly shown in stress-rupture tests on specimens removed before failure. There was a greater reduction in the stress-rupture life for a given number of cycles when the time at T_{max} was increased (compare figs. 2(c) and 9(b)). This effect might mean that the vacancies created by plastic deformation are allowed more time to diffuse together to form cracks.

CONCLUSIONS

The following results and conclusions have been obtained from a study of the effect of exposure to thermal-fatigue conditions on the mechanical properties of ductile alloys:

1. Exposure to thermal-fatigue conditions strengthened one alloy in stress-rupture (S-816) and weakened the other (Inconel 550). Under the most damaging conditions studied, Inconel 550 lost 98 percent of its original stress-rupture life as a result of prior thermal fatigue, even though the number of cycles was only one-half of that required for failure by thermal fatigue alone. Under the same conditions, the stress-rupture life of S-816 was increased about 50 percent.

2. When specimens were first exposed to stress-rupture conditions and then run to failure in thermal fatigue, the thermal-fatigue life of S-816 was sharply reduced, whereas that of Inconel 550 showed a slight increase.

3. The above results can be interpreted by extending existing theories of mechanical fatigue and creep-rupture to thermal fatigue. In this extension the thermal-fatigue process is divided into two stages: first, a stage of strain- and/or precipitation-hardening, during which the ductility is reduced and the strength is increased, and second, a

stage of destruction of cohesive bonds and development and propagation of cracks. Structural changes are an important part of thermal-fatigue behavior.

Lewis Flight Propulsion Laboratory
National Advisory Committee for Aeronautics
Cleveland, Ohio, July 11, 1958

467L

APPENDIX - LITERATURE REVIEW ON MECHANISM OF FAILURE

Results of thermal-fatigue studies emphasize the complexity of the thermal-fatigue process. Many of its features are difficult to incorporate into a working theory, and, in fact, no completely satisfactory theory of thermal fatigue has yet been developed.

This review of the literature is intended to consider those factors in the deformation of metals that may be important in the behavior of materials during reversed deformation under cyclic temperatures. The review starts with theories of low-temperature deformation, and includes brief discussions of the Bauschinger effect, high-temperature creep, and both mechanical and thermal fatigue.

Theory of Deformation

In ductile materials, fracture is preceded by plastic deformation, and this deformation is generally accepted to occur by the movement of dislocations. The deformation is not uniform; certain crystals and planes that are favorably oriented undergo more plastic flow than do other crystals or planes. Additional dislocations are produced during deformation. The dislocations that move through these crystals under stress pile up at grain boundaries and other barriers, where they exert a backward stress. A complex network ("forest") of dislocations results, which opposes the further movement of dislocations, and the material strain-hardens. Its ductility, or ability to absorb further deformation without fracture, is reduced.

Besides deforming by slip along glide planes, some metals and alloys deform by twinning. Nickel alloys, in common with a number of other alloys and metals, are particularly prone to twin formation. Reference 2 proposes that mechanical twinning in alpha-iron is related to the incidence of cleavage fracture and that twinning may on occasion be directly responsible for the onset of cleavage. There are many others who consider mechanical twinning as merely incidental to brittle fracture. Reference 2 gives photomicrographs of recrystallized grains appearing at twin boundaries as evidence of the strained regions about the twins, and postulates that cleavage fracture is initiated when a propagating twin meets an effective barrier and its energy is diverted into producing slip.

Bauschinger Effect

The Bauschinger effect is an important phenomenon in reversed stressing. It is commonly interpreted as follows: The strain in a material that is stressed beyond its elastic limit is not uniform, and certain crystals and planes deform more than others. This sets up residual

strains when the load is released. If the original stress was tensile, some crystals and/or planes become loaded in compression when the tensile load is released. If the material is then loaded in compression, the residual compressive stresses add to the external load, and plastic flow begins at a lower stress than if the material were reloaded in tension.

Zener (ref. 3) suggests that the Bauschinger effect is due to microscopic residual stresses associated with the individual slip bands in the crystals, while others (refs. 4 and 5) attribute it to residual atomic forces around flaws and disordered regions. Heating at relatively low temperatures can provide enough energy for the dislocations or vacancies to diffuse out of these highly strained regions and eliminate the Bauschinger effect.

Theories of Creep

The dislocation model of plastic deformation has been applied to creep at elevated temperatures by assuming that the rate-controlling process for creep consists of the thermal activation of dislocations over barriers. While the main driving force is due to thermal movement, a preferential direction is given by the influence of the applied stress. These ideas have been formalized mathematically by several investigators (ref. 6 and refs. cited therein).

More recently, attention has been directed to the role of vacancies in deformation, particularly in creep at high temperatures. Over-all activation energies for rupture of pure metals that have been computed (ref. 7) are nearly the same as the activation energies for self-diffusion, and vacancies are widely accepted as playing a dominant role in diffusion. At any given temperature, there is an equilibrium number of vacancies that exists within a crystal lattice. Vacant lattice sites in excess of the equilibrium number (and possibly interstitial atoms) are generated by plastic deformation (ref. 8).

The excess of vacancies would tend to revert to the equilibrium amount. At very low strain rates, the concentrations of vacancies would remain substantially at their equilibrium value, whereas at much higher strain rates, larger degrees of supersaturation could be maintained. These ideas are supported by the results of reference 9 on the self-diffusion of alpha-iron at 890°C (1634°F), assuming that diffusion occurs by a vacancy mechanism. The diffusion coefficient increased (linearly) with the strain rate, which was interpreted to mean that the number of vacancies also increased with strain rate, as postulated by Seitz (ref. 8). As a measure of the magnitudes involved, the rate of diffusion at 890°C (1634°F) was increased by a factor of 10 for a strain rate of $0.18\text{ in.}/(\text{in.})(\text{hr})$, which corresponded to a stress of only 1300 psi.

One method for removing excess vacancies and maintaining the equilibrium concentration in a crystal lattice is combining the vacancies, either within the lattice or at the grain boundaries, to form voids. There are several schools of thought as to the mechanism of void formation (refs. 10 to 17), but that which appears most acceptable is nucleation by preexistent nuclei. Reference 15 suggests that the preexistent nuclei may be identified as submicroscopic voids or cracks produced during solidification or working, "supercritical" sized particles containing cracks, or gas pockets. Fissures starting from local regions of high stress concentrations are also thought to influence void formation (refs. 14, 16, and 17).

Numerous investigators have drawn attention to the minute cavities or pores formed in metals undergoing creep at elevated temperatures (refs. 18 to 22). Reference 18 refers to the formation of "distortion cavities" in the grains and grain boundaries of a copper-nickel-silicon alloy as a result of excessive local distortion at discontinuities such as inclusions and particles of a brittle constituent. Reference 21 reports a very thorough study of intergranular cavitation in copper, alpha-brass, and magnesium over a range of strain rates and temperatures. Under the conditions used the disordered lattice at the boundary acted as a trap in which holes readily formed. The crystal lattice was a continuous source of vacancies, generated by dislocation motion, and the grain-boundary cavities were continuous sinks.

Cavitation appeared more readily under conditions that caused a change in emphasis from deformation by slip to deformation by grain translation (i.e., lower strain rates and higher temperatures), though this might have been a cause rather than an effect. Thus, a sliding movement at the grain boundaries would probably cause localized distortion of the lattice that would aid cavities in forming, whereas, on the other hand, the nucleation of large numbers of cavities would weaken the boundaries and therefore aid movement in those regions. As deformation proceeded, more vacancies would be absorbed by the existing cavities, and these would grow in size. The cavities would also be spread by tensile stress concentrations. Their growth, coupled with the applied stress, would ultimately cause the cavities in a boundary to link together. The grains would then part and an intercrystalline crack would be formed.

Mechanical Fatigue

In many respects thermal fatigue is similar to mechanical fatigue, and one can reasonably expect that the mechanism for high-temperature mechanical fatigue will, with some modification, apply also to thermal fatigue.

A number of theories have appeared through the years to explain the failure of metals by fatigue (refs. 23 to 27). While most of them have

long been discarded, they all agree that the fatigue of metals is associated with a slip process similar to that involved in unidirectional extension. This, references 26 and 27 report that the same slip planes and slip directions operated for both repeated cyclic stressing and monotonic loading, and that fatigue was invariably accompanied by evidence of strain-hardening. Slip bands developed early under cyclic stressing and were accompanied by strain-hardening, but they did not cause cracks to form so long as the stresses were below the endurance limit. At stresses above the endurance limit cracks formed in the regions of slip, and additional slip bands continued to form and broaden even after fatigue cracks had appeared. Single crystals and polycrystalline specimens both appeared to behave in the same manner, although there were differences in degree which were associated with grain boundaries that acted to inhibit slip and influenced the rate of propagation of fatigue cracks.

The reversed straining in thermal fatigue has been pictured as due to the movement of dislocations back and forth from one barrier to another with each stress reversal (ref. 28). A certain amount of energy is required to generate the dislocations and to move them back and forth from barrier to barrier; this energy is continuously dissipated into the lattice as thermal vibration and is responsible for the hysteresis loop found under cyclic stressing. Certain factors cause this process to be irreversible and cause it to move to neighboring planes so that the region of dislocation reversal grows.

The quantitative theory of fatigue presented in 1939 by Orowan (ref. 29) considers local plastic slip and subsequent strain-hardening as the principal cause of fatigue and assumes that a fatigue failure occurs when the "total plastic strain" (i.e., the sum of the absolute values of all positive and negative strains) reaches a characteristic finite value. The argument proceeds as follows:

(1) Stress distribution is more or less inhomogeneous in all materials because of the unavoidable presence of small cracks and structural inhomogeneities (e.g., grain boundaries and inclusions) as well as inhomogeneities created by plastic flow.

(2) If the material is brittle, fracture occurs when the stress at the point where the stress concentration is highest reaches the true strength of the material.

(3) If the material is plastic, it will yield at the stress peaks (i.e., at the points where local maxima of stress occur) before the true strength is reached. Further increase of load causes more plastic strain at these points, but the stress does not increase appreciably beyond the yield point. The surplus stress is taken over by the (more or less elastic) surroundings of the stress peak, and, in this way, the stress distribution is smoothed out.

(4) If the load is alternating, the local plastic yielding will not come to an end but will alternate, and this will produce a progressive strain-hardening at the stress peaks. Consequently, the stress at which plastic yielding begins increases in the course of the load fluctuations, the smoothing out of the stress distribution becomes less effective, and the maximum stress at the stress peaks rises until finally a crack is formed when the stress reaches the strength of the materials.

(5) For plastic materials, the condition of fracture can be regarded as the attainment of either a critical stress (the strength) or a critical strain. In alternating deformation, the total strain (i.e., the sum of the absolute values of all positive and negative strains suffered in the course of the stress cycles) has a characteristic value at fracture, provided that there is no considerable strain-hardening recovery.

(6) The plastic strain amplitudes of consecutive cycles decrease approximately as the terms of a geometric series; thus, the total strain produced by an infinite number of cycles is always finite without respect to whether the strength is finite or not. If this limiting value of the total plastic strain is smaller than the critical strain, failure will not occur.

After sufficient cycling, a fatigue crack is produced in a region of intense slip. The mechanism for the crack formation is not clear, but it must ultimately depend upon the concentration of the reversed dislocation motion on certain planes. Reference 28 suggests that it is due to a running together of dislocations as they are halted at the barriers. Reference 30 suggests that it is due to a clustering together of the lattice vacancies generated by the dislocation motion.

Reference 29 emphasizes that the treatment therein deals with the formation of the fatigue crack, not with its propagation to complete fracture of the specimen. The propagation of a crack is assumed to take place by plastic deformation and progressive fracture at the growing tip. Therefore, whether a fatigue crack forms early or late in the fatigue life, the ease or difficulty of dislocation movement is likely to exert a controlling influence (ref. 31).

One should also note that the plastic distortion caused by cyclic stressing is not necessarily damaging, as evidenced by the phenomenon of "understressing," which increases the fatigue strength at subsequent higher stress cycles. Moreover, the progress of the distortion, as observed by microscopic slip lines or by X-ray diffraction studies, is not necessarily a measure of crack formation, particularly in the early stages of fatigue, but may be due to mere cold-working (strain-hardening) of the material.

4671

CA-3

Observations in reference 32 on the fatigue behavior of high-strength aluminum alloys suggest that precipitation-hardening alloys are unstable under cyclic stresses, which cause precipitation or overaging in the localized regions of intense deformation. Although the static strength as a whole may not be impaired, the localized bands of precipitation produced by cyclic stressing are regions of low strength in which fatigue cracks form. Thus, the amount of precipitation-hardening and the relative stability of the precipitates are important factors to be considered.

Reference 33 contends that fatigue is not inseparably associated with plastic slip, but that the real fatigue effect is a large-scale expression of the progressive destruction of cohesive bonds in the material. Plastic deformation and strain-hardening are assumed to be essential features only insofar as they modify both the intensity and rate of bond destruction. According to reference 33, the destruction of the cohesive bonds cannot be satisfactorily detected in what appears to be undamaged material by a metallographic examination of slip lines, by hardness, or by X-ray diffraction studies of submicroscopic lattice breakdown. Long before any submicroscopic crack can be observed, fatigue has already been initiated by the severance of a number of cohesive bonds. The assumptions that the "separation strengths" of the cohesive bonds have a statistical distribution and that the stress caused by an applied load varies inhomogeneously within the material are the basis for the statistical treatment of reference 33.

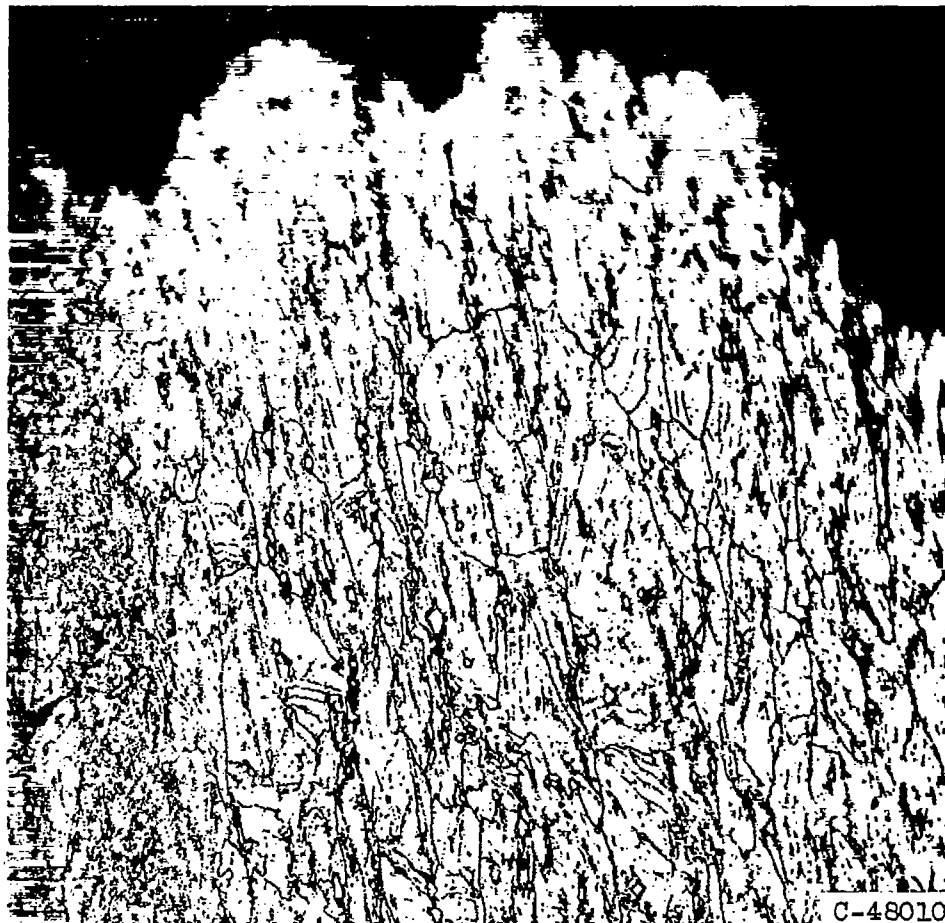
REFERENCES

1. Clauss, Francis J., and Freeman, James W.: Thermal Fatigue of Ductile Materials. I - Study of the Effect of Variations in the Temperature Cycle on the Thermal-Fatigue Life of S-816 and Inconel 550. NACA TN 4160, 1958.
2. Bruckner, W. H.: The Micromechanism of Fracture in Ferrite. *Acta Metall.*, vol. 2, Jan. 1954, pp. 168-169.
3. Zener, Clarence: Elasticity and Anelasticity of Metals. Univ. Chicago Press, 1948, p. 146.
4. Elsesser, T. M., Sidebottom, O. M., and Corten, H. T.: The Influence of Aging on the Bauschinger Effect in Inelastically Strained Beams. *Trans. ASME*, vol. 74, Nov. 1952, pp. 1291-1296.
5. Corten, H. T., and Elsesser, T. M.: The Effect of Slightly Elevated-Temperature Treatment Upon Microscopic and Submicroscopic Residual Stresses Induced by Small Inelastic Strains in Metals. *Trans. ASME*, vol. 74, Nov. 1952, pp. 1297-1302.

- 4671
- CA-3 back
6. Orowan, E.: The Creep of Metals. Jour. West Scotland Iron and Steel Inst., vol. 54, Feb. 1947, pp. 45-96.
 7. Sherby, Oleg D., Orr, Raymond L., and Dorn, John E.: Creep Correlations of Metals at Elevated Temperatures. Trans. AIME, vol. 200, Jan. 1954, pp. 71-80.
 8. Seitz, F.: On the Generation of Vacancies by Moving Dislocations. Advances in Phys., vol. 1, Jan. 1952, pp. 43-90.
 9. Buffington, F. S., and Cohen, M.: Self-Diffusion in Alpha Iron under Uniaxial Compressive Stress. Trans. AIME, vol. 194, 1952, pp. 859-860.
 10. Seitz, F.: On the Porosity Observed in the Kirkendall Effect. Acta Metall., vol. 1, no. 3, May 1953, pp. 355-369.
 11. Baes, C. F., Jr., and Kellogg, H. H.: The Effect of Dissolved Sulfur on the Surface Tension of Liquid Copper. Trans. AIME, vol. 197, 1953, pp. 643-648.
 12. Balluffi, R., and Seigle, L.: Effect of Grain Boundaries upon Pore Formation and Dimensional Changes During Diffusion. Acta Metall., vol. 3, no. 2, Mar. 1955, pp. 170-177.
 13. Balluffi, R.: The Supersaturation and Precipitation of Vacancies During Diffusion. Acta Metall., vol. 2, no. 2, Mar. 1954, pp. 194-202.
 14. Seigle, L., and Resnick, R.: On Pore Formation During Diffusion. Acta Metall., vol. 3, Nov. 1955, pp. 605-606.
 15. Machlin, E. S.: Creep-Rupture by Vacancy Condensation. Trans. AIME, vol. 206, Feb. 1956, pp. 106-111.
 16. Brinkman, J. A.: Mechanism of Pore Formation Associated with the Kirkendall Effect. Acta Metall., vol. 3, no. 2, Mar. 1955, pp. 140-145.
 17. Brinkman, J. A.: On the Mechanism of Pore Formation During Diffusion. Acta Metall., vol. 3, Nov. 1955, pp. 606-607.
 18. Jenkins, C. H. M., Bucknall, E. H., and Jenkinson, E. A. The Inter-Relation of Age-Hardening and Creep Performance. II - The Behaviour in Creep of an Alloy Containing 3 Percent Nickel and Silicon in Copper. Jour. Inst. Metals, vol. 70, Feb. 1944, pp. 57-79.

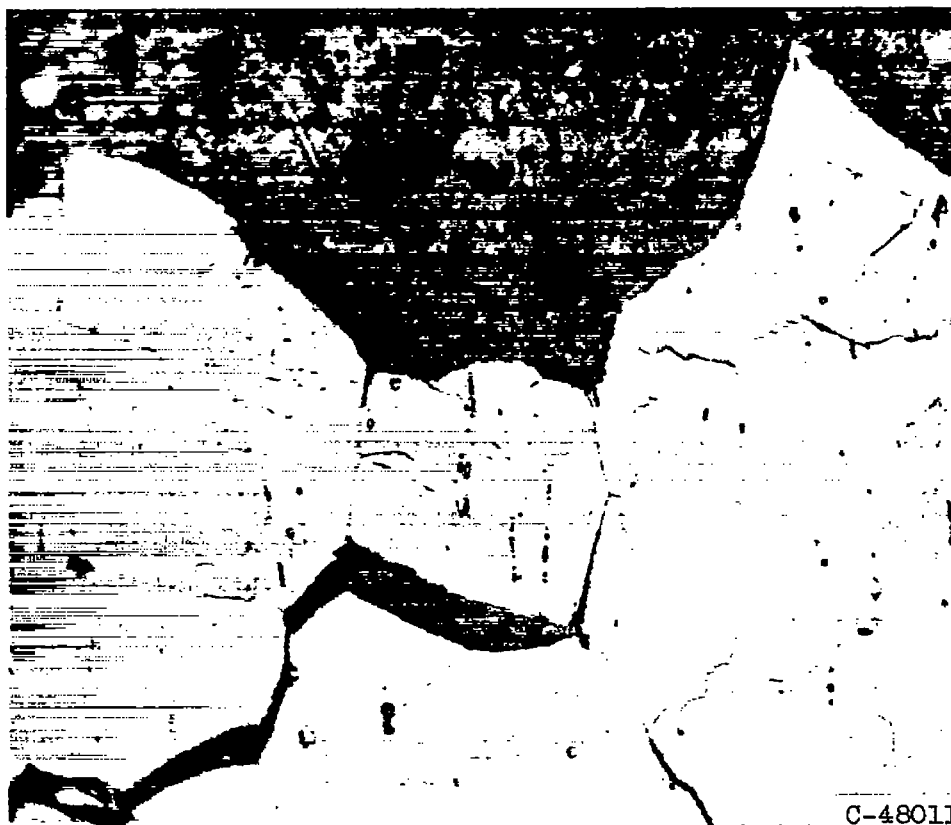
19. Whitaker, Marjorie E.: Intercrystalline Failure of Brasses and Aluminum Brasses in Air, Ammonia, and Certain Aqueous Solutions and Molten Metals. *Metallurgia*, vol. 39, no. 229, Nov. 1948, pp. 21-29. (See also vol. 39, no. 230, Dec. 1948, pp. 66-70.)
20. Benson, N. D., McKeown, J., and Mends, D. N.: The Creep and Softening Properties of Copper for Alternator Rotor Windings. *Jour. Inst. Metals*, vol. 80, Nov. 1951, pp. 131-142.
21. Greenwood, J. Neill, Miller, D. R., and Suiter, J. W.: Intergranular Cavitation in Stressed Metals. *Acta Metall.*, vol. 2, no. 2, Mar. 1954, pp. 250-258.
22. Guy, A. G.: Russian Theory for Creep Fracture. *Metal Prog.*, vol. 69, no. 3, Mar. 1956, pp. 158; 160-162.
23. Ewing, J. A., and Hunfrey, J. C. W.: The Fracture of Metals under Repeated Alternations of Stress. *Phil. Trans. Roy. Soc. (London)*, vol. 200, 1903, p. 241.
24. Beilby, G. T.: The Hard and Soft States in Ductile Metals. *Proc. Roy. Soc. (London)*, vol. 79, ser. A, 1907, p. 463.
25. Beilby, G. T.: The Hard and Soft States in Metals. *Jour. Inst. Metals*, vol. 6, 1911, pp. 5-43.
26. Gough, H. J.: Crystalline Structure in Relation to Failure of Metals - Especially by Fatigue. *Proc. ASTM*, vol. 33, pt. 2, 1933, pp. 3-114.
27. Gough, H. J., and Wood, W. A.: A New Attack upon the Problem of Fatigue of Metals, Using X-Ray Methods of Precision. *Proc. Roy. Soc. (London)*, vol. 154, no. A833, May 1936, pp. 510-539.
28. Coffin, L. F., Jr.: A Study of the Effects of Cyclic Thermal Stresses on a Ductile Material. *Trans. ASME*, vol. 76, Aug. 1954, pp. 931-949; discussion, pp. 949-950.
29. Orowan, E.: Theory of the Fatigue of Metals. *Proc. Roy. Soc. (London)*, ser. A, vol. 171, 1939, pp. 79-106.
30. Wood, W. A., and Davis, R. B.: Effects of Alternating Strain on the Structure of a Metal. *Proc. Roy. Soc. (London)*, vol. 220, ser. A, Nov. 10, 1953, pp. 255-266.
31. Broom, T., Molineux, J. H., and Whittaker, V. N.: Structural Changes During the Fatigue of Some Aluminum Alloys. *Jour. Inst. Metals*, vol. 84, 1955-1956, pp. 357-363.

32. Hanstock, R. F.: Fatigue Phenomena in High-Strength Aluminum Alloys. Jour. Inst. Metals, vol. 83, 1954-1955, pp. 11-15.
33. Freudenthal, A. M.: The Statistical Aspect of the Fatigue of Materials. Proc. Roy. Soc. (London), vol. 187, ser. A, Dec. 13, 1946, pp. 416-429.



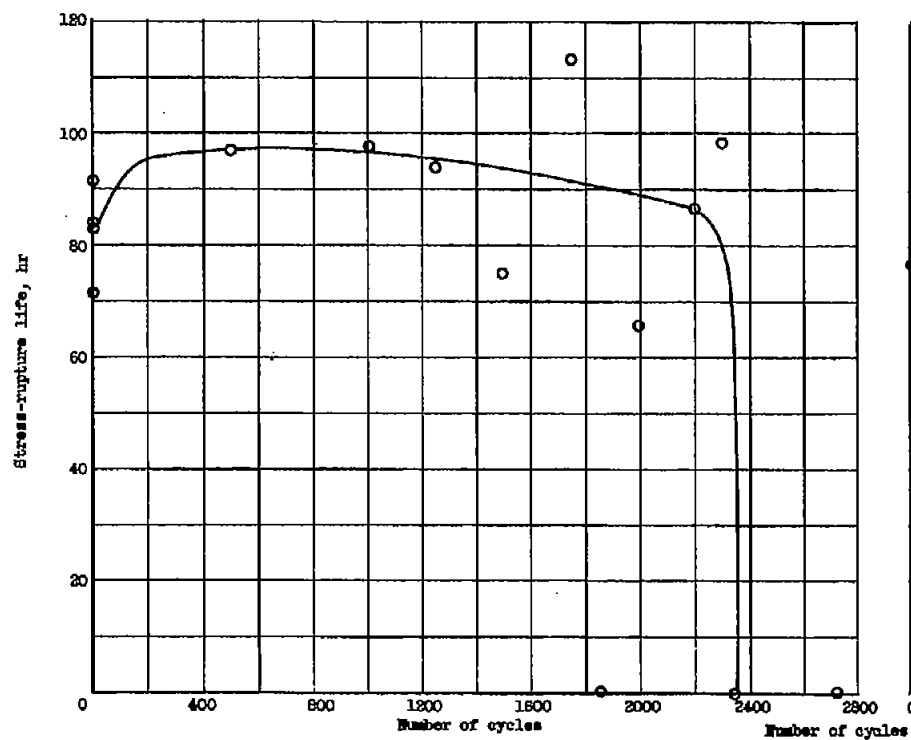
(a) S-816 fractured after 77.4 hours at 40,000 psi. Electrolytically etched in solution of aqua regia and glycerol.

Figure 1. - Microstructures of heat-treated specimens fractured in stress-rupture at 1350° F. X250.

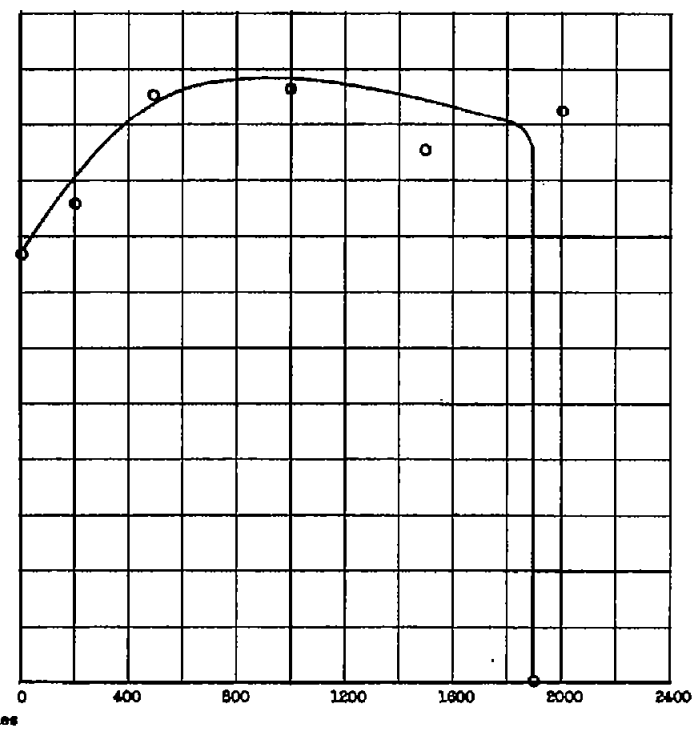


(b) Inconel 550 fractured after 213.9 hours at 56,500 psi. Electrolytically etched in dilute solution of hydrofluoric acid and glycerol in water.

Figure 1. - Concluded. Microstructures of heat-treated specimens fractured in stress-rupture at 1350° F. X250.

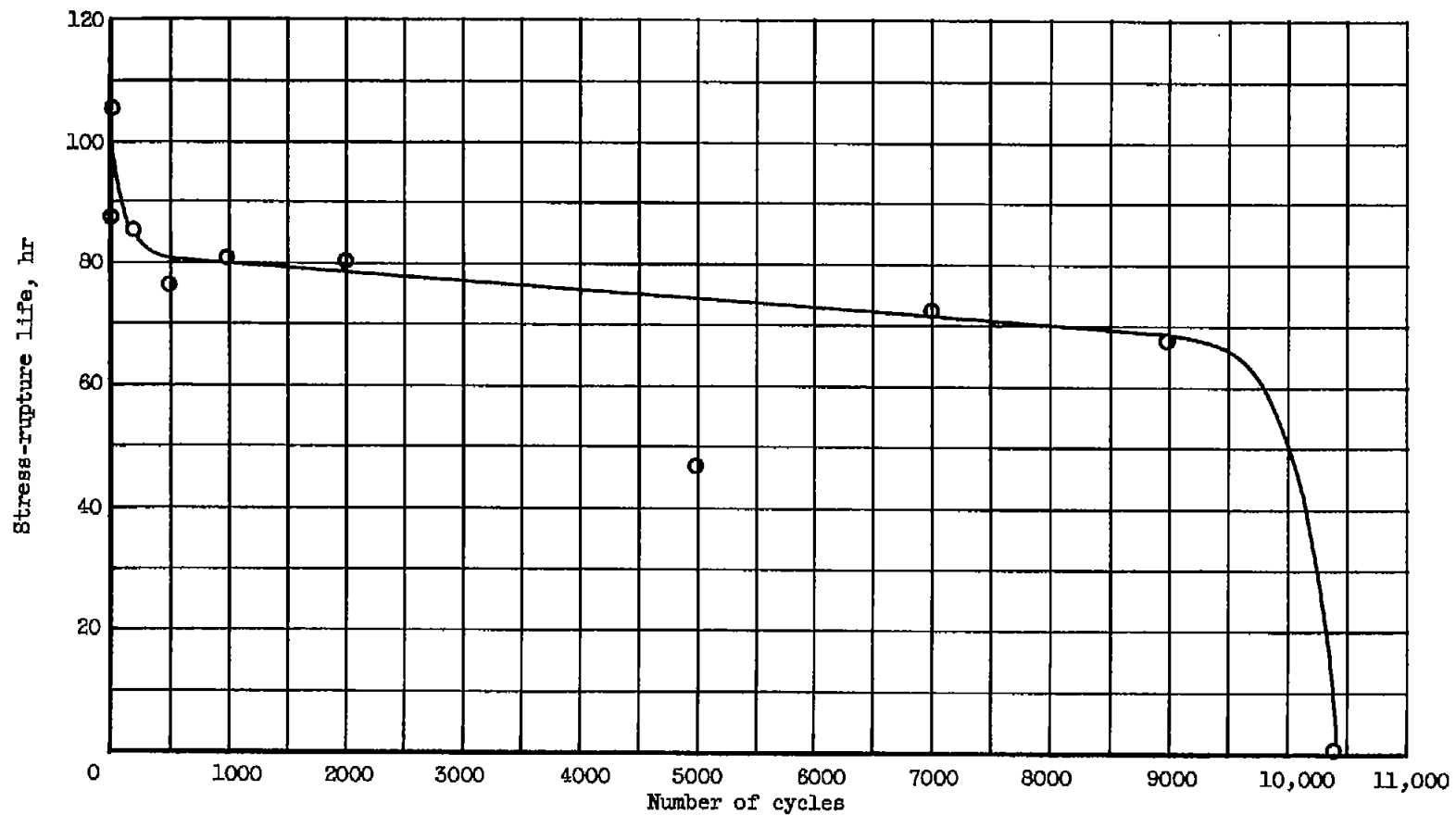


(a) S-816 at 40,000 psi and 1350° F.



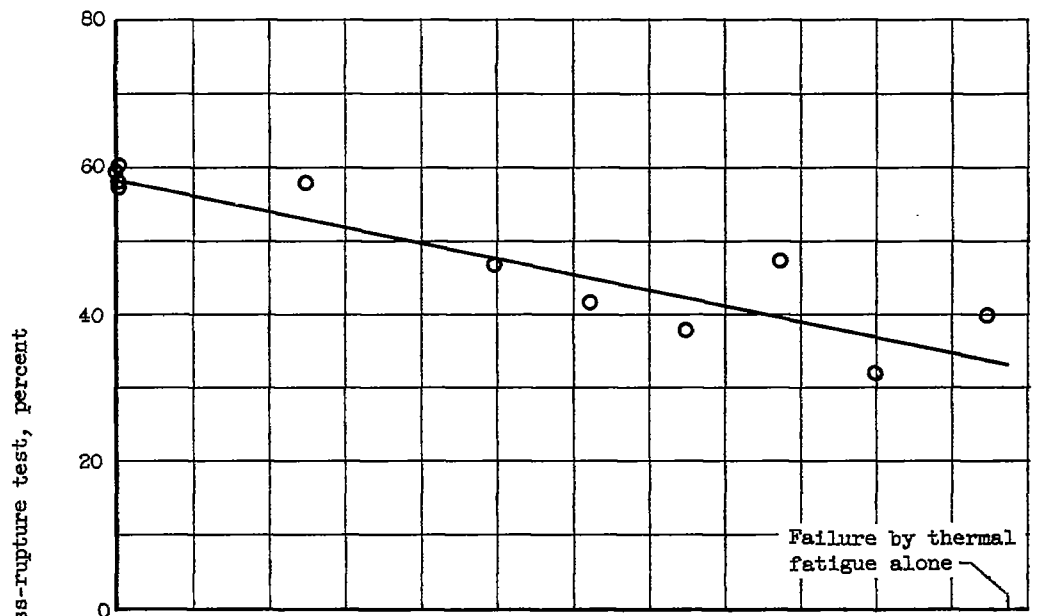
(b) S-816 at 25,000 psi and 1500° F.

Figure 2. - Effect of prior thermal cycling with 15 seconds at maximum temperature on stress-rupture life. Maximum cycling temperature, 1350° F; minimum cycling temperature, 200° F; clamped at 1350° F, unclamped at 200° F; 30 seconds of heating or cooling; 15 seconds at temperature.

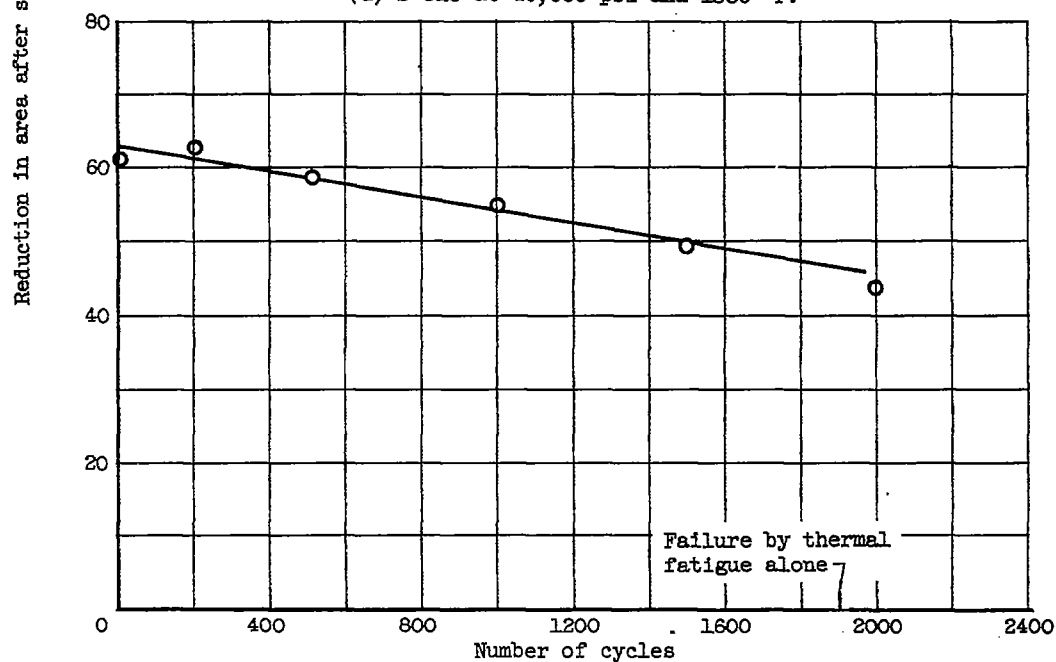


(c) Inconel 550 at 56,500 psi and 1350° F.

Figure 2. - Concluded. Effect of prior thermal cycling with 15 seconds at maximum temperature on stress-rupture life. Maximum cycling temperature, 1350° F; minimum cycling temperature, 200° F; clamped at 1350° F, unclamped at 200° F; 30 seconds of heating or cooling; 15 seconds at temperature.

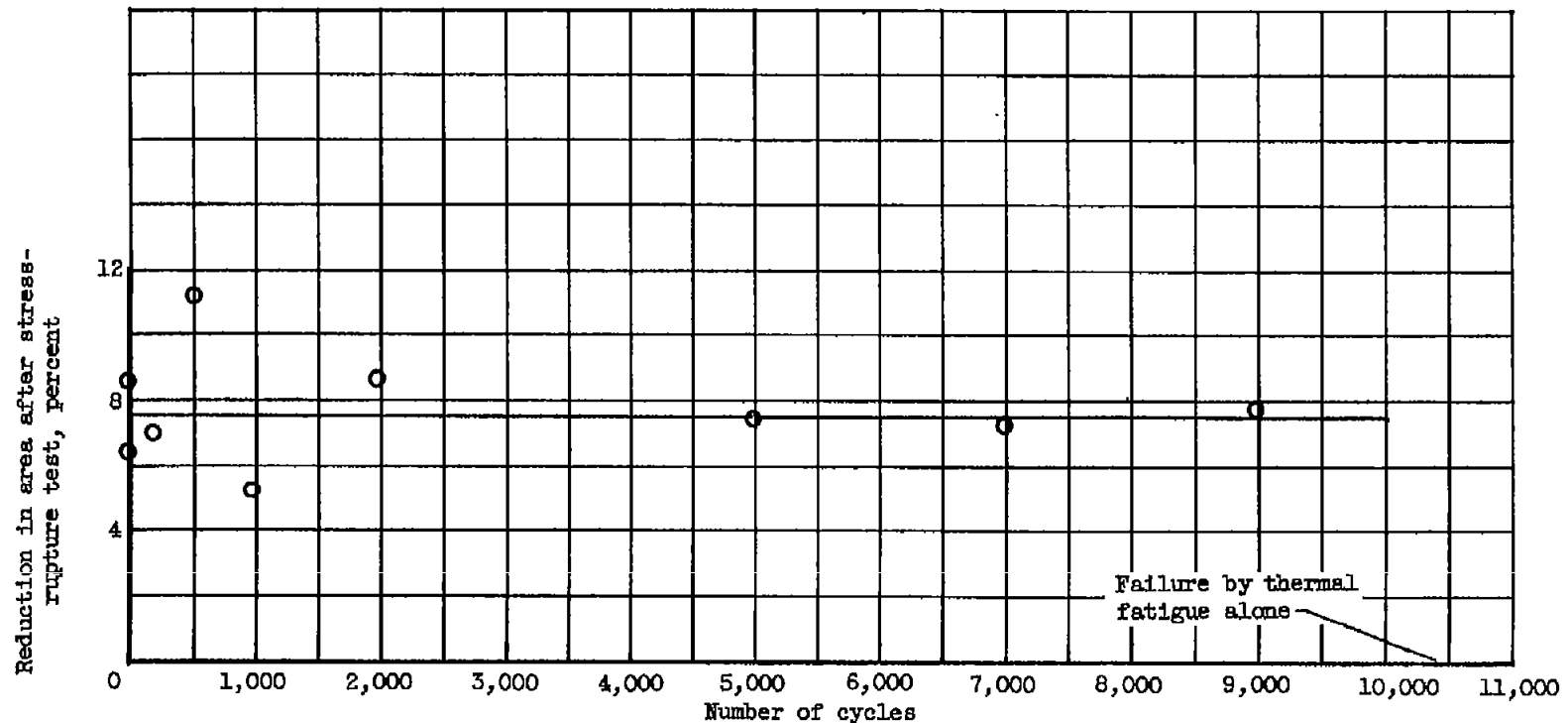


(a) S-816 at 40,000 psi and 1350° F.



(b) S-816 at 25,000 psi and 1500° F.

Figure 3. - Effect of prior thermal cycling with 15 seconds at maximum temperature on stress-rupture ductility. Maximum cycling temperature, 1350° F; minimum cycling temperature, 200° F; clamped at 1350° F, unclamped at 200° F; 30 seconds of heating or cooling; 15 seconds at temperature.



(c) Inconel 550 at 56,500 psi and 1350° F.

Figure 3. - Concluded. Effect of prior thermal cycling with 15 seconds at maximum temperature on stress-rupture ductility. Maximum cycling temperature, 1350° F; minimum cycling temperature, 200° F; clamped at 1350° F, unclamped at 200° F; 30 seconds of heating or cooling; 15 seconds at temperature.

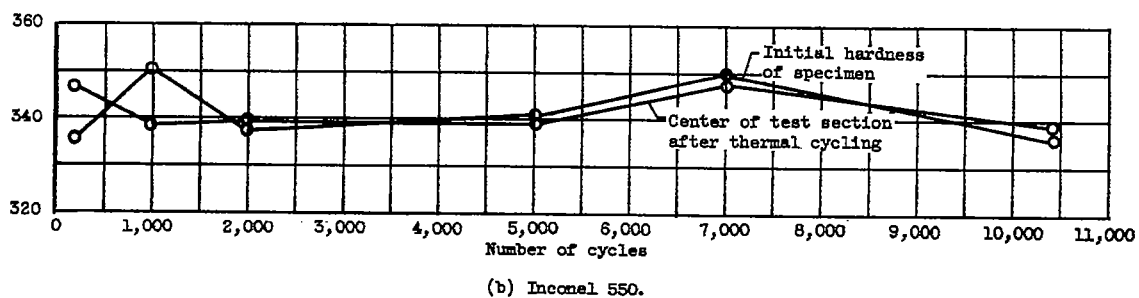
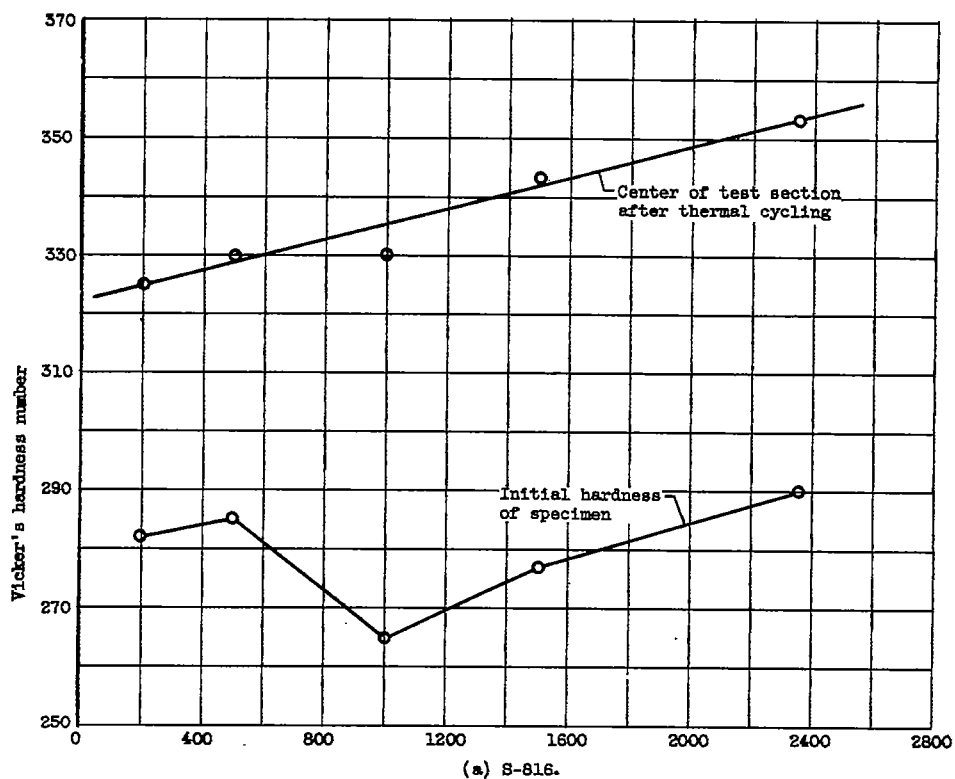
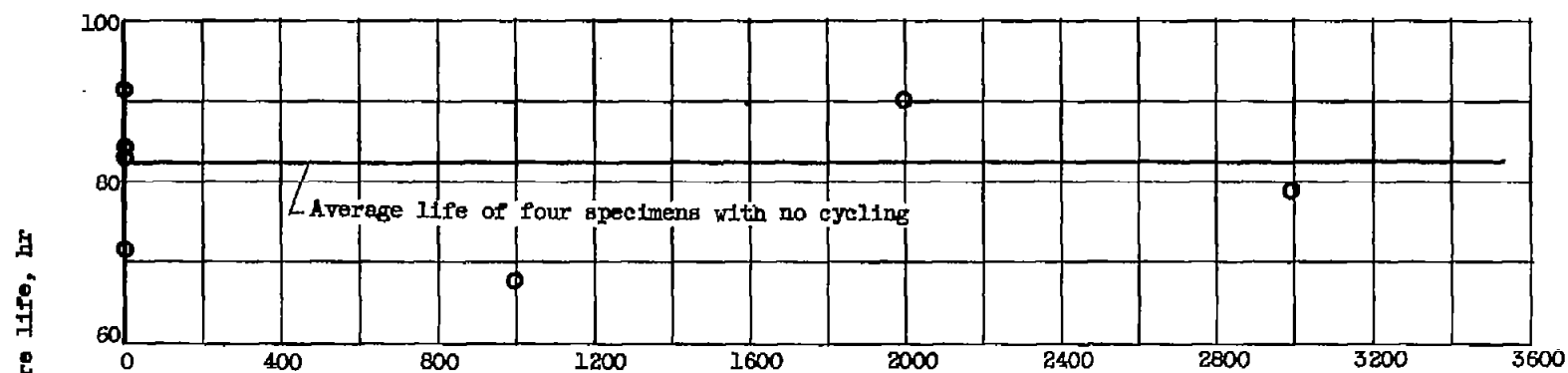
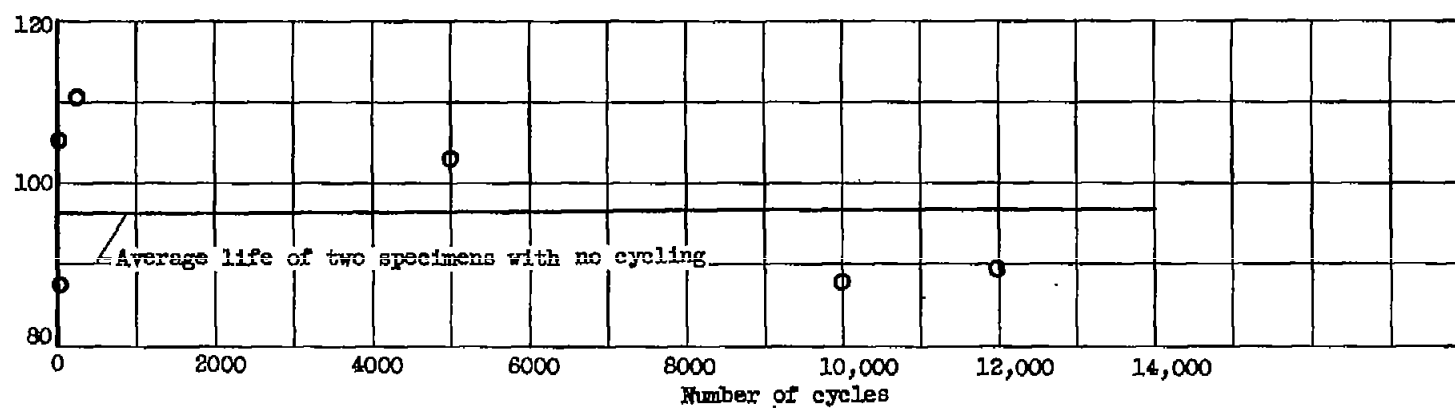


Figure 4. - Effect of thermal cycling on hardness. Maximum cycling temperature, 1350° F; minimum cycling temperature, 200° F; clamped at 1350° F, unclamped at 200° F; 30 seconds of heating or cooling; 15 seconds at temperature.



(a) S-816 at 40,000 psi.



(b) Inconel 550 at 56,500 psi.

Figure 5. - Effect of prior thermal cycling without constraint on stress-rupture life at 1350° F. Maximum cycling temperature, 1350° F; minimum cycling temperature, 200° F.

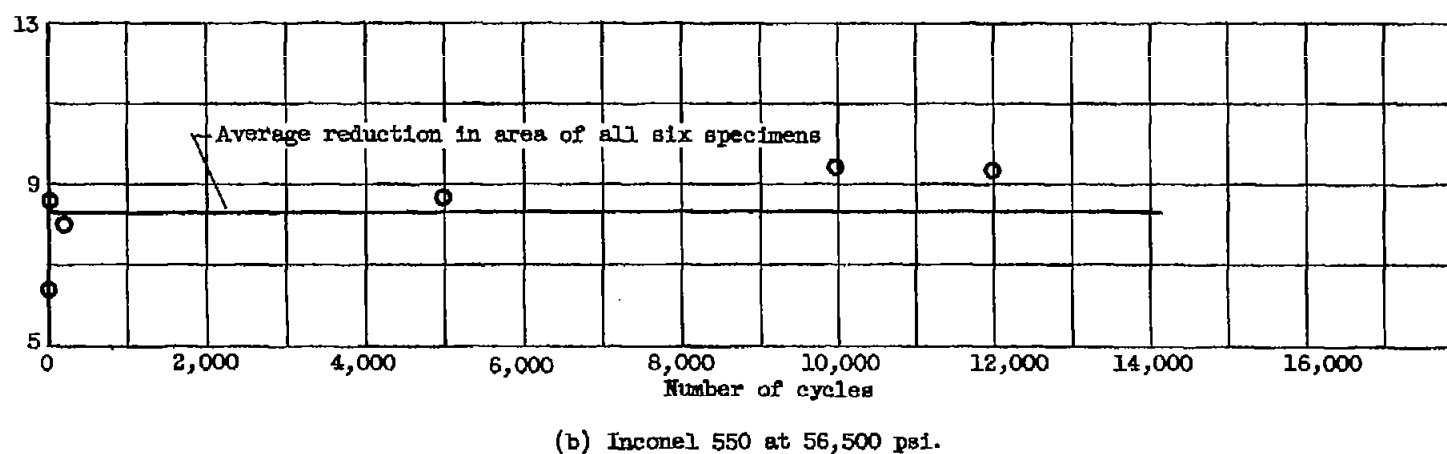
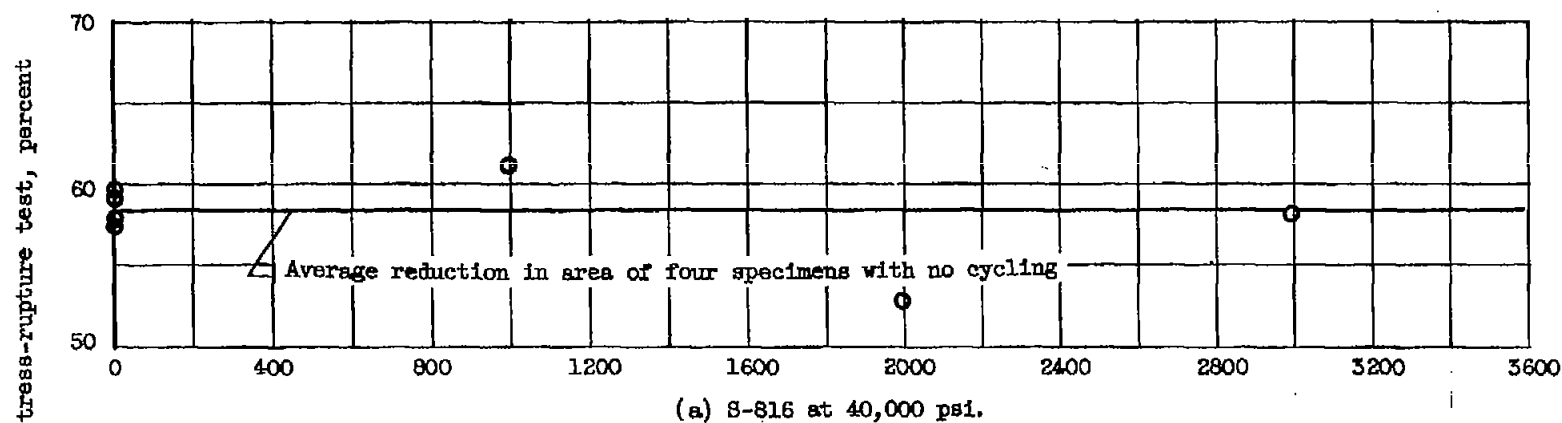
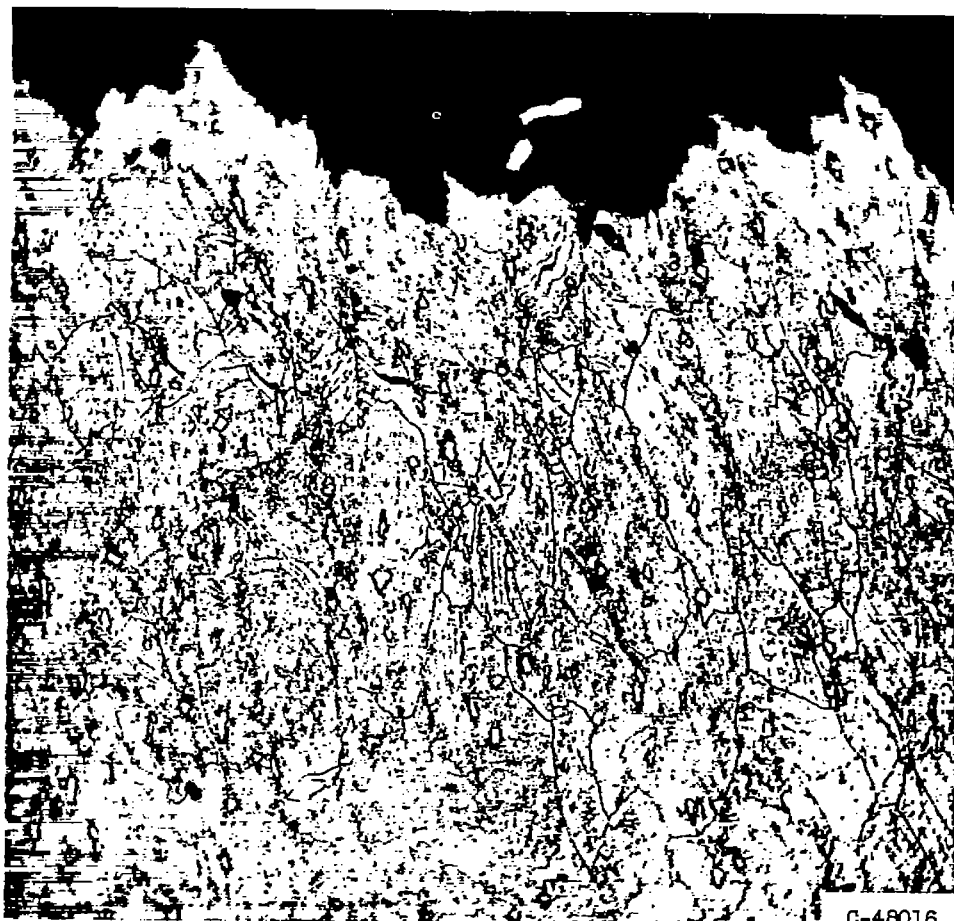
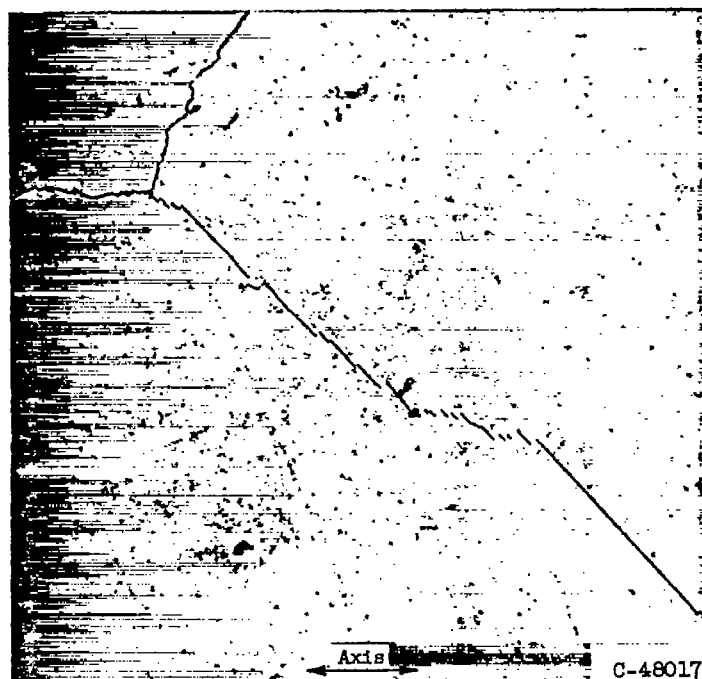


Figure 6. - Effect of prior thermal cycling without constraint on stress-rupture ductility at 1350° F. Maximum cycling temperature, 1350° F; minimum cycling temperature, 200° F; 30 seconds of heating or cooling; 15 seconds at temperature.

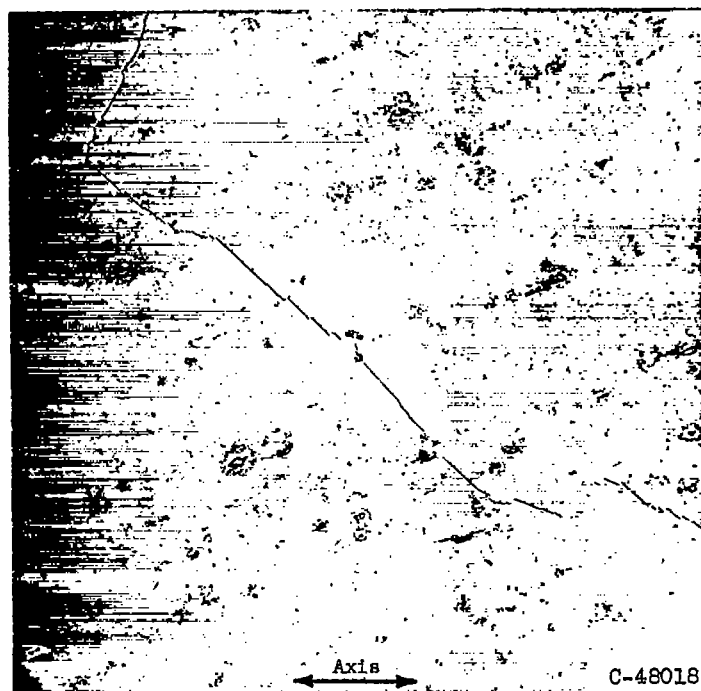


C-48016

Figure 7. - Microstructure of S-816 specimen that had been cycled 1175 times in thermal fatigue between 1350° and 200° F and then fractured in stress-rupture after 115.3 hours at 40,000 psi and 1350° F. Electrolytically etched in solution of aqua regia and glycerol. X250.



(a) 1000 Cycles. X750.

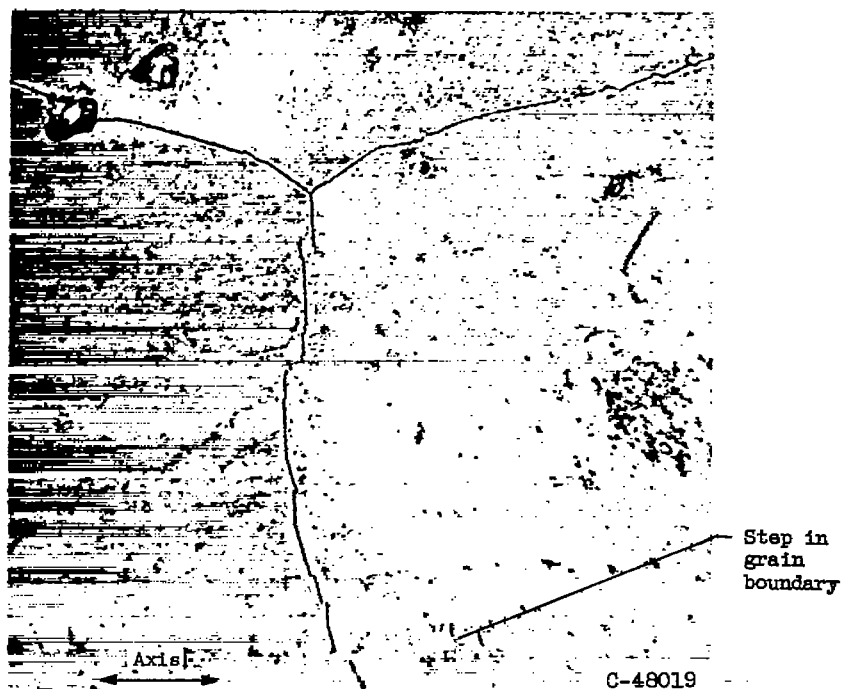


(b) 1000 Cycles. X220.

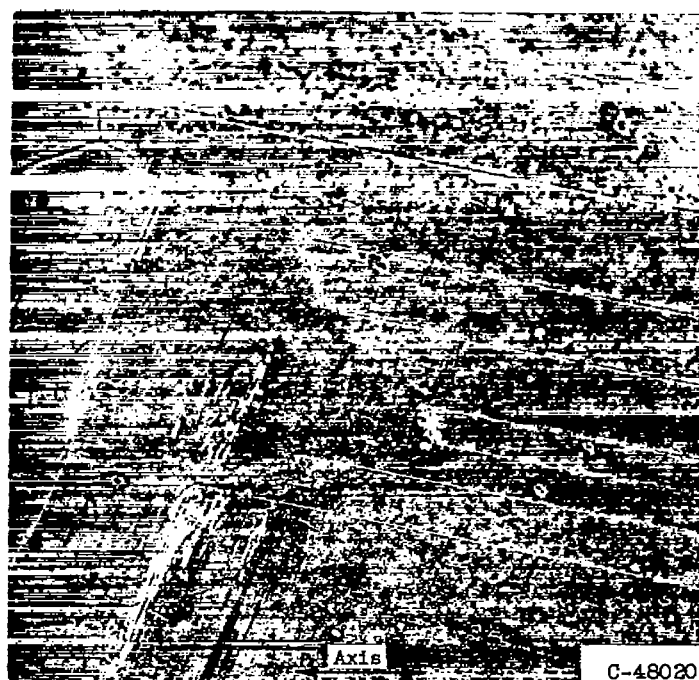
Figure 8. - Microstructure of Inconel 550 after thermal cycling between 1350° and 200° F. Electrolytically etched in dilute solution of hydrofluoric acid and glycerol in water. (Pictures reduced 74 percent in reproduction.)

4671

CA-5

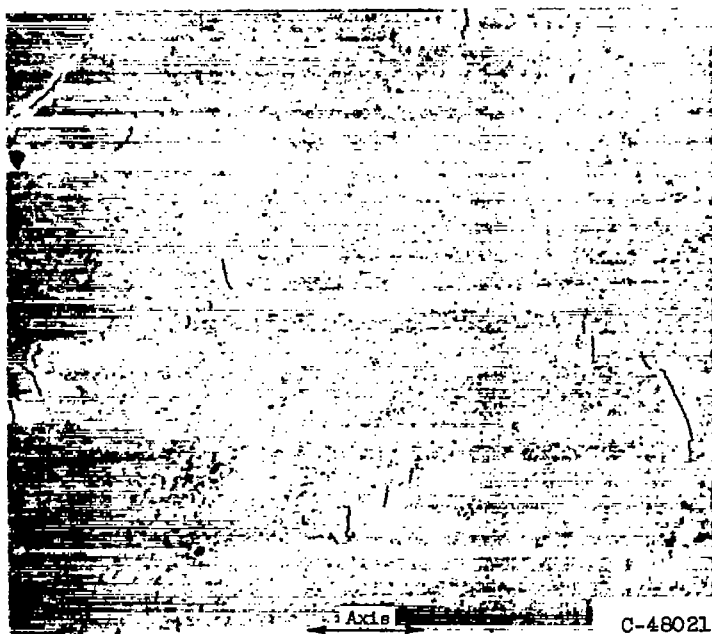


(c) 7000 Cycles. X750.

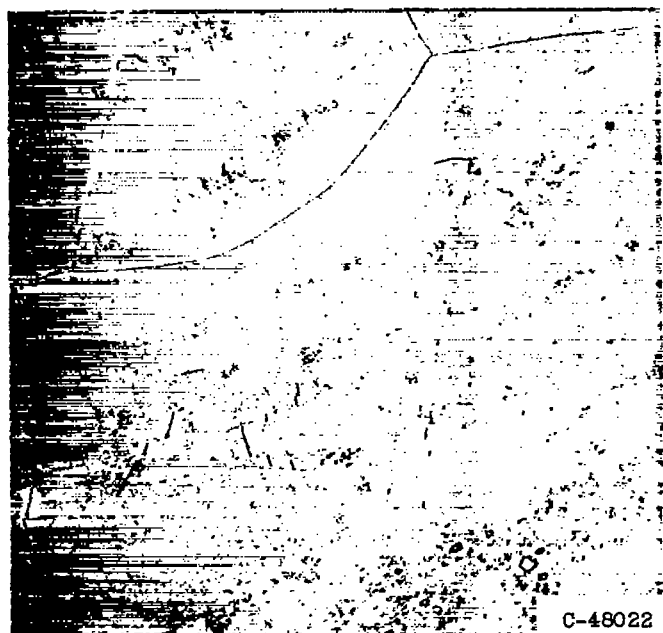


(d) 2000 Cycles. X250.

Figure 8. - Continued. Microstructure of Inconel 550 after thermal cycling between 1350° and 200° F. Electrolytically etched in dilute solution of hydrofluoric acid and glycerol in water. (Pictures reduced 74 percent in reduction.)

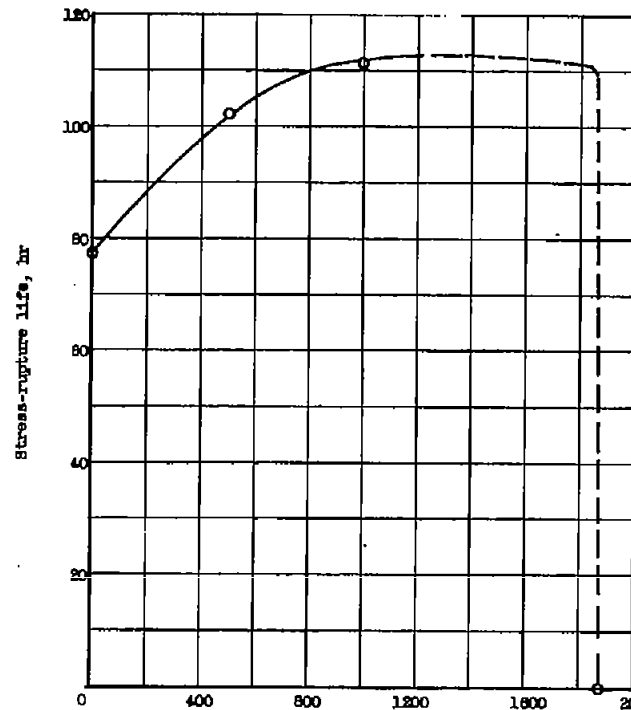


(e) 7000 Cycles. X750.

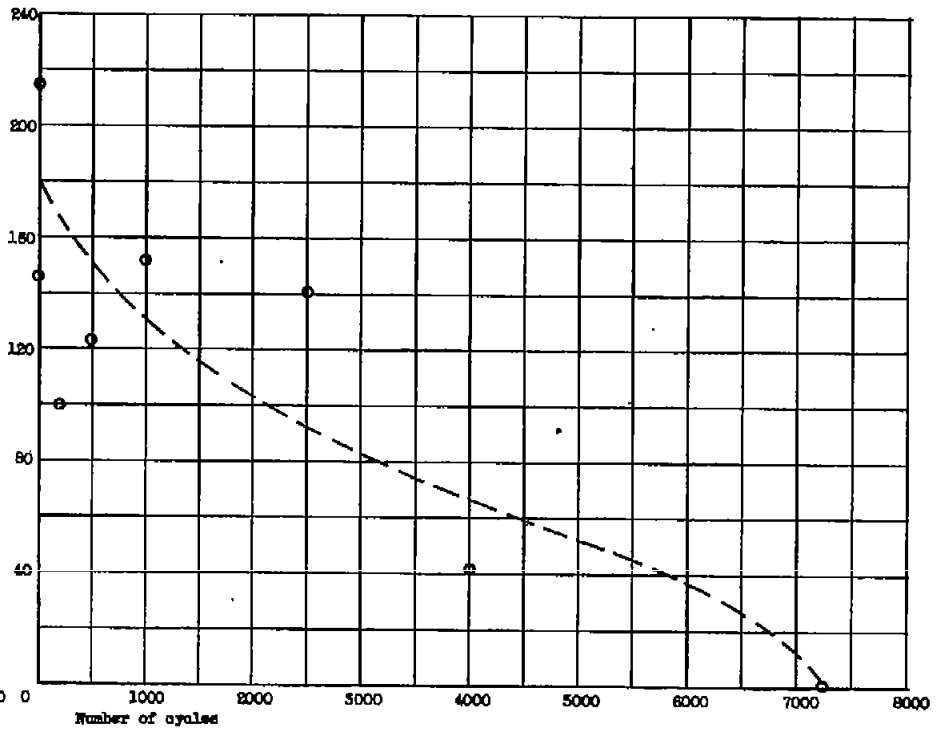


(f) 7000 Cycles. X500.

Figure 8. - Concluded. Microstructure of Inconel 550 after thermal cycling between 1350° and 200° F. Electrolytically etched in dilute solution of hydrofluoric acid and glycerol in water. (Pictures reduced 74 percent in reproduction.)



(a) S-816 at 40,000 psi.



(b) Inconel 560 at 56,500 psi.

Figure 9. - Effect of prior thermal cycling with 60 seconds at maximum temperature on stress-rupture life at 1350° F. Maximum cycling temperature, 1350° F; minimum cycling temperature, 200° F; 30 seconds of heating, 60 seconds at 1350° F, 30 seconds of cooling, 15 seconds at 200° F.

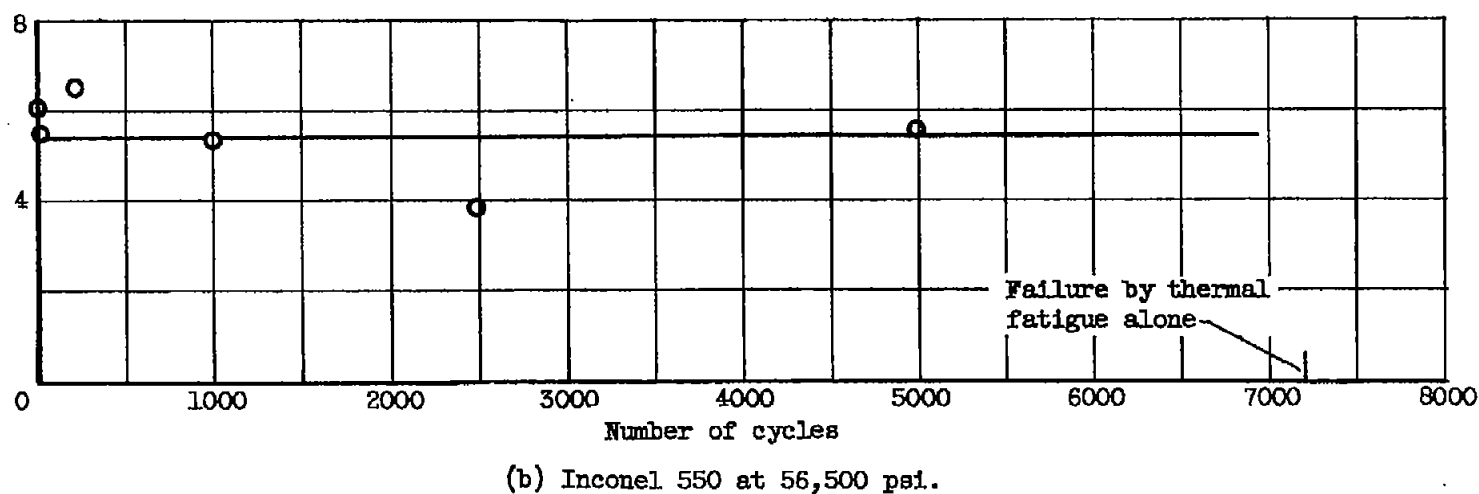
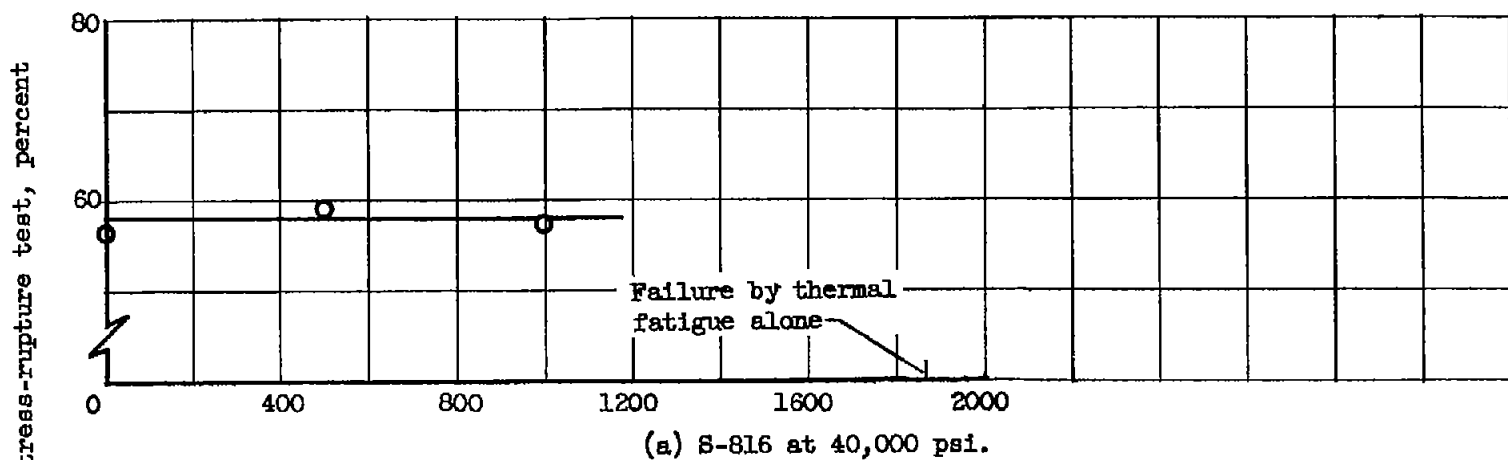
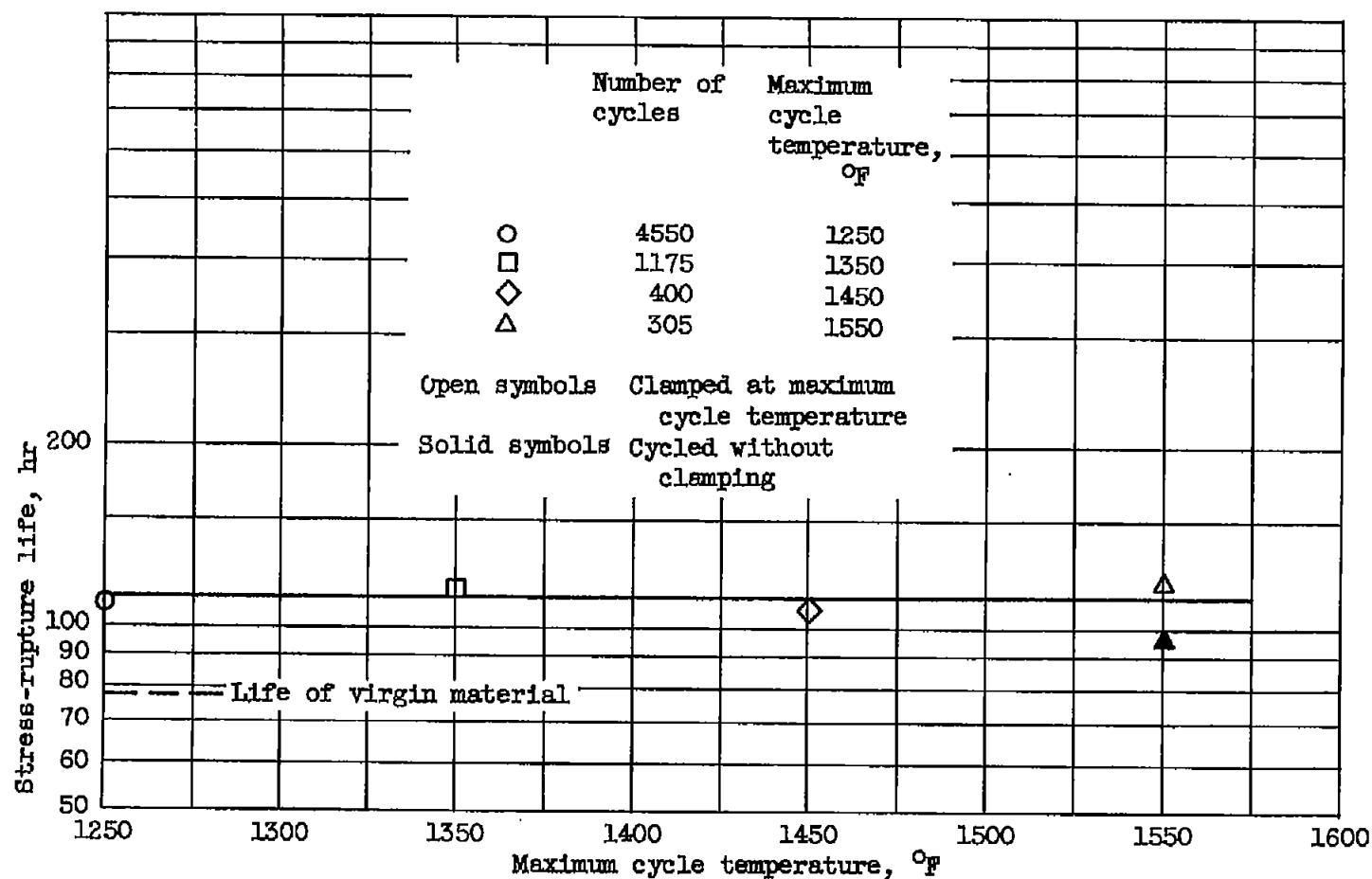
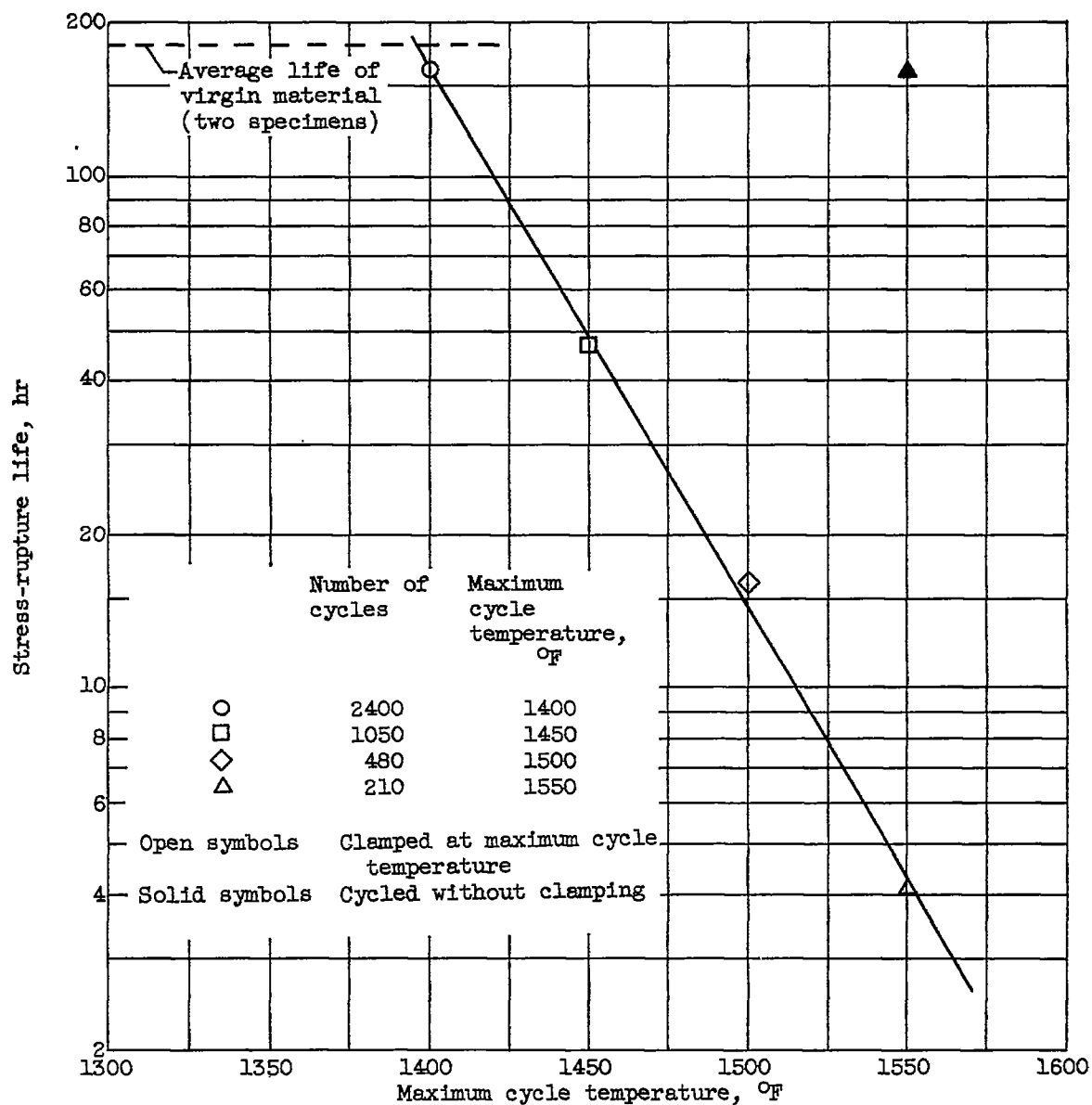


Figure 10. - Effect of prior thermal cycling with 60 seconds at maximum temperature on stress-rupture ductility at 1350° F. Maximum cycling temperature, 1350° F; minimum cycling temperature, 200° F; 30 seconds of heating, 60 seconds at 1350° F, 30 seconds of cooling; 15 seconds at 200° F.



(a) S-816 at 40,000 psi.

Figure 11. - Effect of maximum cycle temperature of thermal cycling on stress-rupture life at 1350° F. Minimum cycle temperature, 200° F; 30 seconds of heating or cooling; 15 seconds at temperature; number of cycles, one-half that for failure by thermal fatigue alone.



(b) Inconel 550 at 56,500 psi.

Figure 11. - Concluded. Effect of maximum cycle temperature of thermal cycling on stress-rupture life at 1350° F. Minimum cycle temperature, 200° F; 30 seconds of heating or cooling; 15 seconds at temperature; number of cycles, one-half that for failure by thermal fatigue alone.

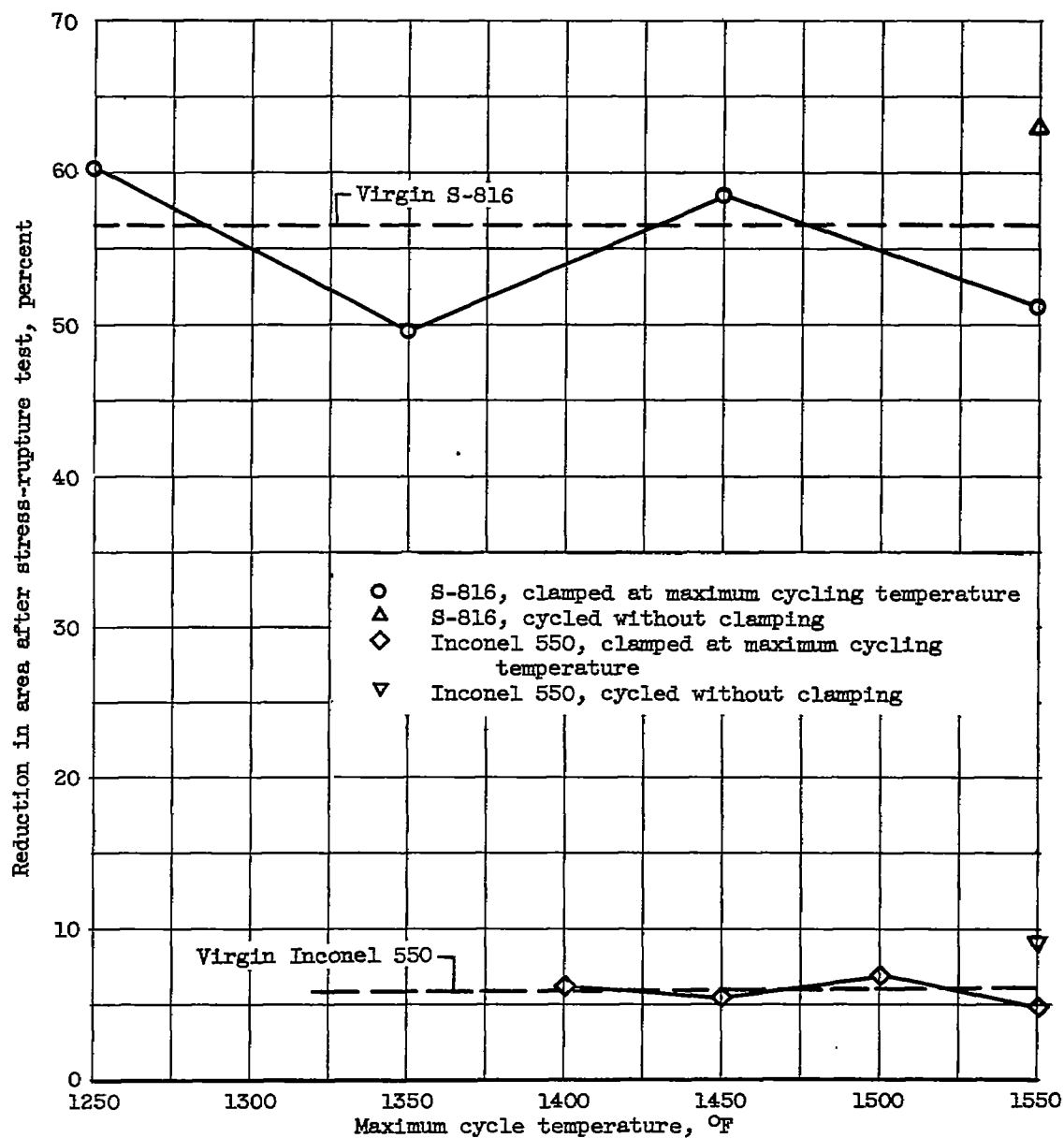
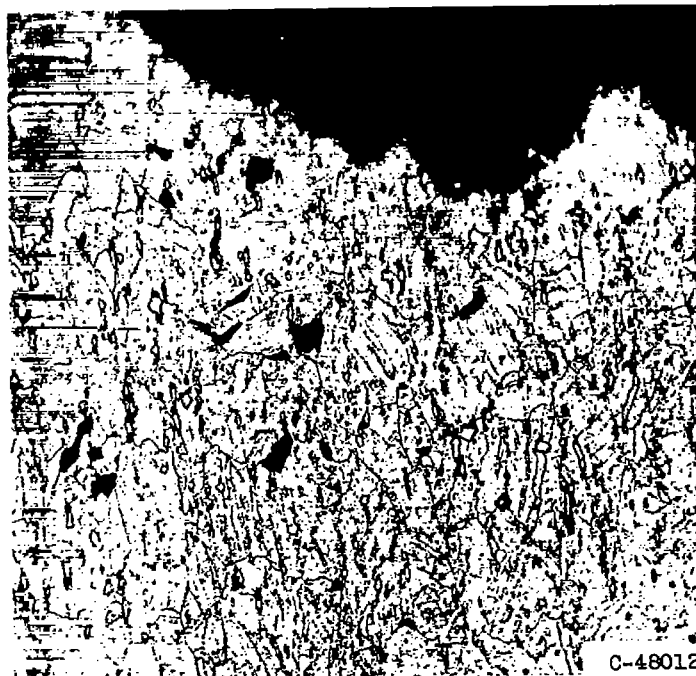
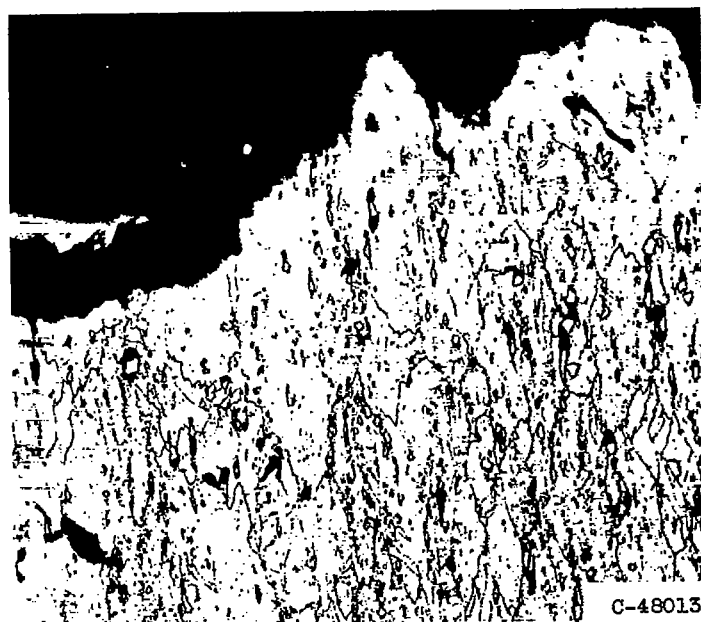


Figure 12. - Effect of maximum temperature of thermal cycling on stress-rupture ductility of S-816 and Inconel 550 at 1350° F. Minimum cycle temperature, 200° F; 30 seconds of heating or cooling; 15 seconds at temperature; number of cycles, half that for failure by thermal fatigue alone.



(a) Fracture after 117.2 hours.

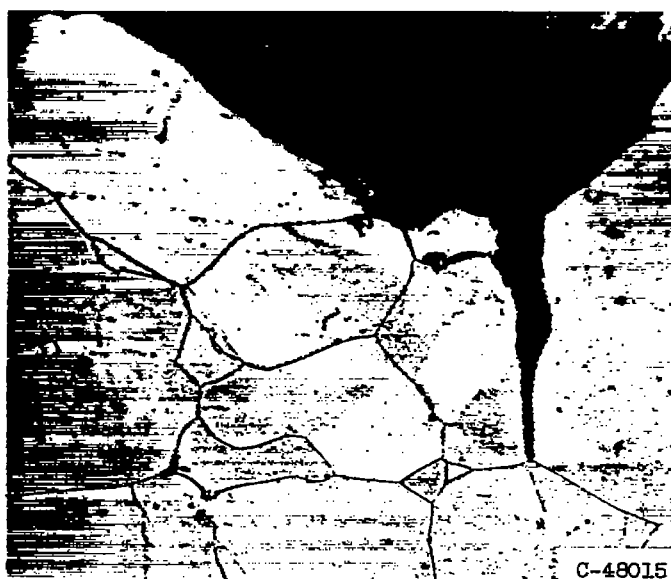


(b) No constraint during thermal cycling; fracture after 95.4 hours.

Figure 13. - Microstructure of S-816 specimen that had been cycled 305 times between 1550° and 200° F and then fractured in stress-rupture at 40,000 psi and 1350° F. Electrolytically etched in solution of aqua regia and glycerol. X250. (Pictures reduced 74 percent in reduction.)

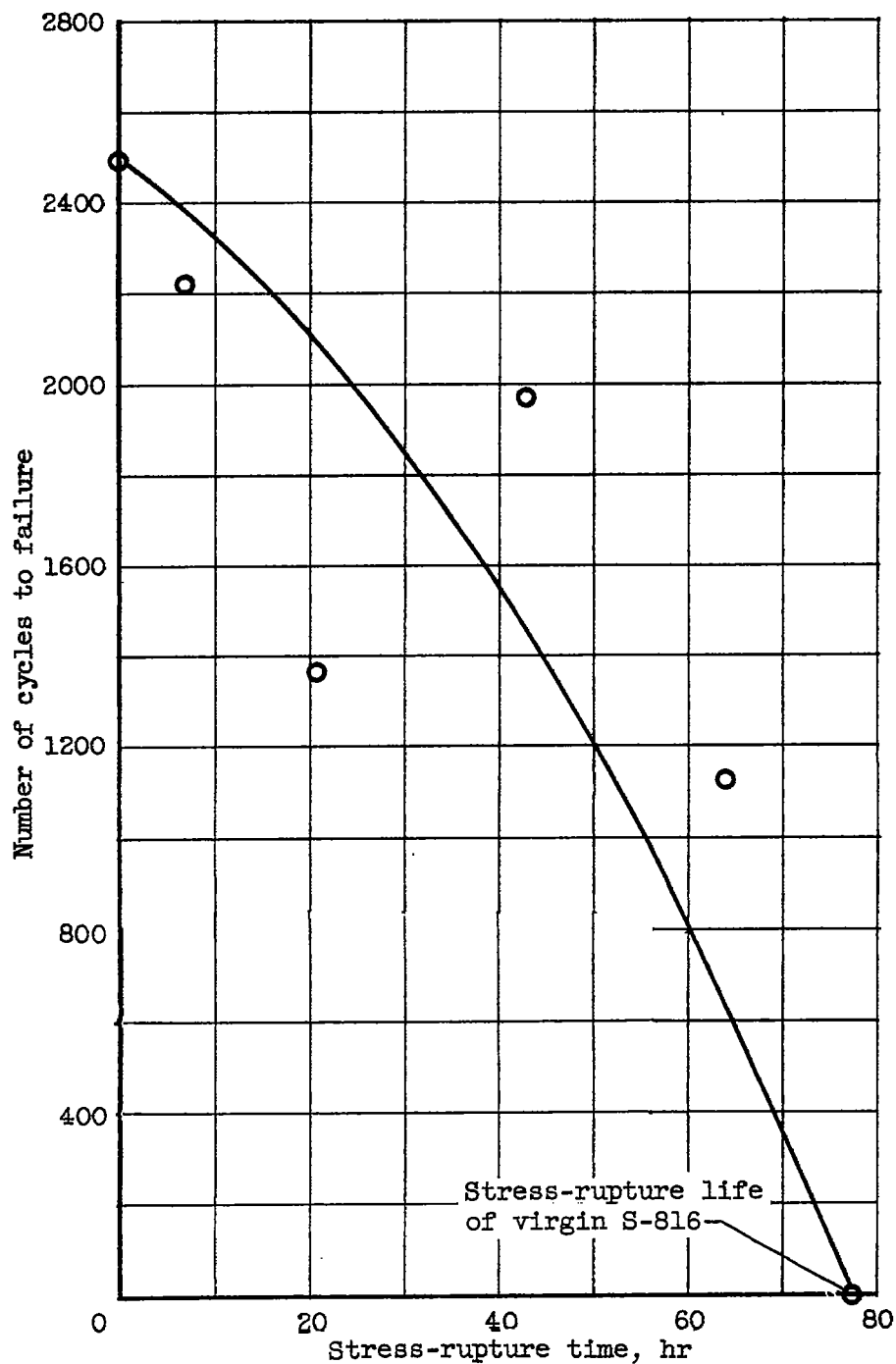


(a) Fracture after 4.08 hours.



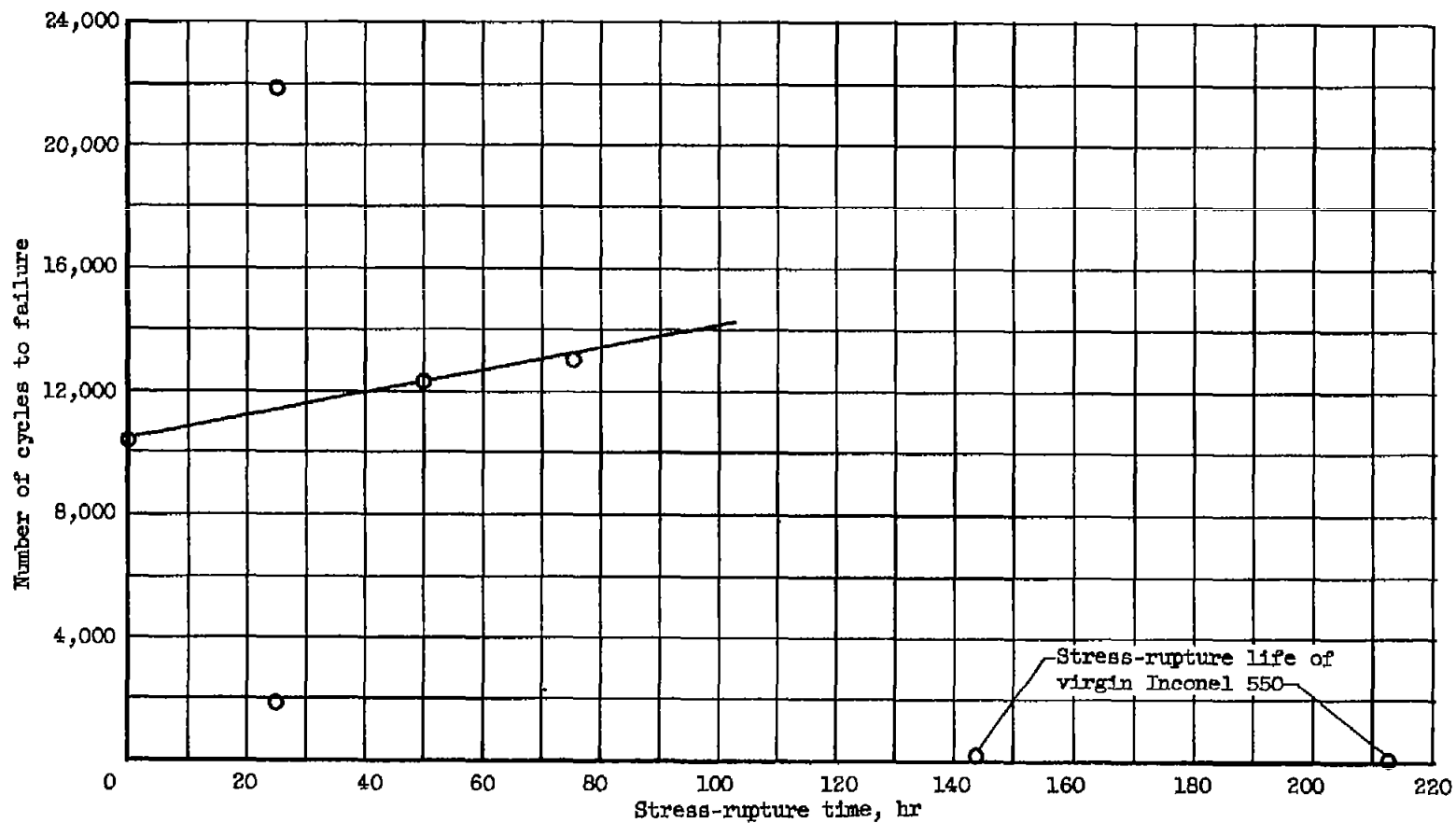
(b) No constraint during thermal cycling; fracture after 159.0 hours.

Figure 14. - Microstructure of Inconel 550 specimen that had been cycled 210 times between 1550° and 200° F and then fractured in stress-rupture at 56,500 psi and 1350° F. Electrolytically etched in dilute solution of hydrofluoric acid and glycerol in water. X250. (Pictures reduced 71 percent in reproduction.)



(a) S-816 stressed at 40,000 psi during stress-rupture.

Figure 15. - Effect of exposure to stress-rupture at 1350° F on subsequent thermal-fatigue life for cycling between 1350° and 200° F on 30-15-30-15-second cycle.



(b) Inconel 550 stressed at 58,500 psi during stress-rupture.

Figure 15. - Concluded. Effect of exposure to stress-rupture at 1350° F on subsequent thermal-fatigue life for cycling between 1350° and 200° F on 30-15-30-15-second cycle.